Mineral. Soc. Amer. Spec. Pap. **2**, 217–239 (1969).

METAMORPHIC PYROXENES AND AMPHIBOLES IN THE BIWABIK IRON FORMATION, DUNKA RIVER AREA, MINNESOTA[1]

BILL BONNICHSEN

Department of Geological Sciences, Cornell University, Ithaca, New York 14850

ABSTRACT

The Dunka River area is at the eastern end of Minnesota's Mesabi range where the Biwabik Iron Formation lies unconformably on older granitic rocks and has been intruded and metamorphosed to the pyroxene hornfels facies by mafic rocks of the overlying Duluth Complex. The metamorphism was isochemical, except for loss of the original H_2O and CO_2.

During metamorphism the original carbonates and phyllosilicates in the iron formation were converted to pyroxenes and fayalite. Orthopyroxene, Ca pyroxene, fayalite, cummingtonite, and hornblende are abundant; the amphiboles formed mainly from pyroxenes during retrograde metamorphism. Quartz and magnetite are the most abundant minerals just as they were prior to metamorphism. The O^{18}/O^{16} ratios of coexisting quartz and magnetite imply that the maximum contact temperature in the rocks underlying the Duluth Complex was 700°–750°C.

Orthopyroxene is the most abundant ferromagnesian silicate, most is ferrohypersthene; in rocks with high Fe/(Mg + Fe) ratios it coexists with fayalite plus quartz. Part crystallized initially as orthopyroxene but a significant portion, occurring in rocks with sufficient iron, crystallized initially as pigeonite and inverted to orthopyroxene during cooling. The temperature of the orthopyroxene-pigeonite phase boundary varies markedly with changes in the Fe/(Mg + Fe) ratio; for Mg-rich compositions typical of mafic igneous rocks it is at magmatic temperatures, whereas for the Fe-rich compositions encountered in the iron formation it intersects the fayalite plus quartz compositional field at less than 700°–750°C. Orthopyroxene grains are disproportionately larger than associated minerals; this probably results from a high nucleation energy

Most of the cummingtonite is paragenetically late; it developed from ferrohypersthene mainly, and from fayalite. Prismatic cummingtonite commonly replaced ferrohypersthene on a volume-for-volume basis; the reaction was similar to: (orthopyroxene + $2H^+ \rightarrow$ cummingtonite + Fe^{2+}), in which the Mg/Si ratio was preserved. Later generations of cummingtonite have developed by other reactions; SiO_2 and iron were consumed in some and liberated in others.

INTRODUCTION

The Dunka River area is at the eastern end of the Mesabi range in northeastern Minnesota, a few miles east of the town of Babbitt (Fig. 1). In this area the Biwabik Iron Formation has been metamorphosed to the pyroxene hornfels facies by mafic intrusive rocks of the overlying Duluth Complex.

Other than erosion and moderate tilting which accompanied the intrusion of the Duluth Complex, the iron formation has remained virtually undisturbed since the time of metamorphism. The area is moderately well exposed by natural outcrops and the geology is even more accessible because of the mining activity and extensive diamond drilling. Portions of the iron formation which contain sufficient magnetite are mined in an open pit by Erie Mining Co. The iron formation in the area offers unparalleled opportunities for the detailed examination of mineralogic and chemical relationships among pyroxenes, amphiboles and olivine which have formed under comparatively well-known conditions.

This paper deals with the detailed petrographic and chemical relationships among the coexisting pyroxenes, amphiboles, and olivine in the Dunka River area. It is drawn from a broader field and laboratory investigation of the general geology and petrology of the Biwabik Iron Formation in the area that was initiated by the writer in 1963 (Bonnichsen, 1968).

[1] Contribution No. 526, Department of Geological Sciences, Cornell University, Ithaca, N.Y. 14850

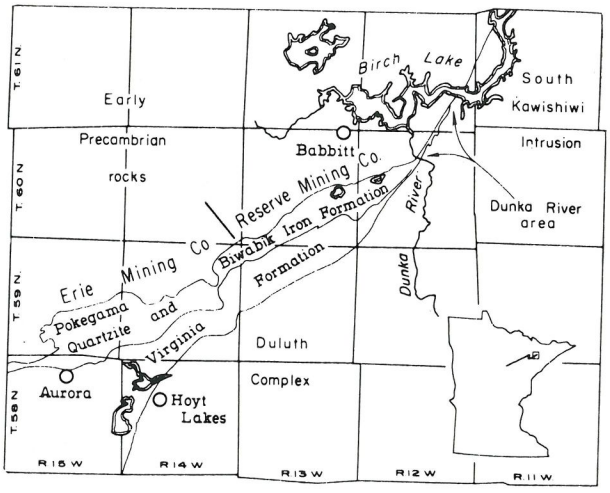

FIG. 1. Index map of the Eastern Mesabi district showing the location of the Dunka River area in relation to other features in the region.

Geology. Three major ages of Precambrian rocks are present in northeastern Minnesota; these include the metamorphosed and folded volcanic and sedimentary rocks and granitic plutons of the Early Precambrian, the Animikie Group of the Middle Precambrian, and the Keweenawan rocks of the Late Precambrian. The Biwabik Iron Formation is the middle formation of the Animikie Group; it conformably overlies the Pokegama Quartzite and is overlain conformably by the Virginia Formation, a thick sequence of black and grey argillite (White, 1954).

The Animikie Group rests unconformably on the underlying Early Precambrian rocks and commonly dips 5° to 10° to the

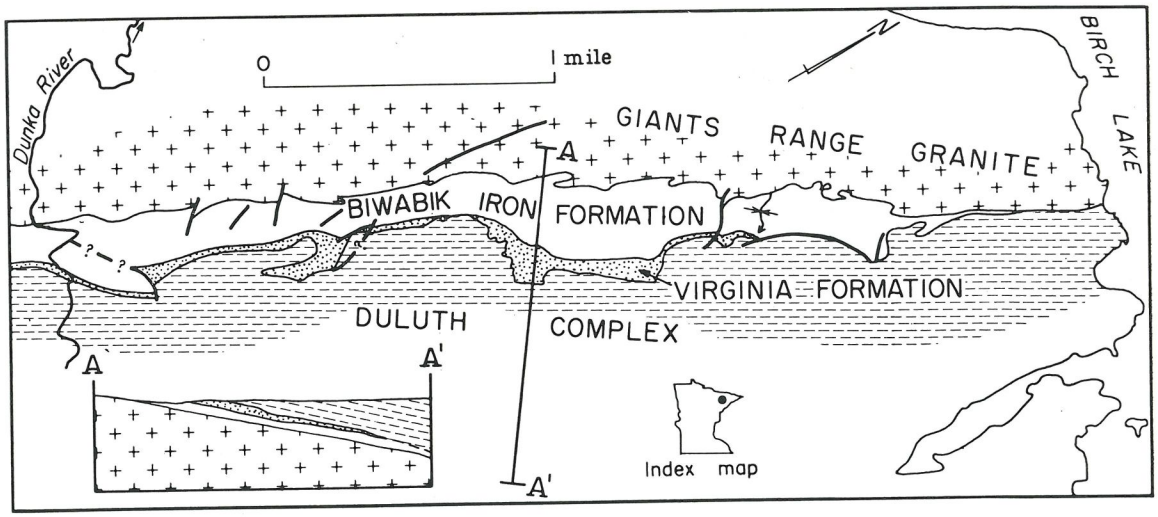

FIG. 2. Geologic map and cross-section of the Dunka River area, St. Louis County, Minnesota.

south or southeast. The Animikie rocks are truncated to the east by the Keweenawan mafic intrusive rocks of the Duluth Complex. The Dunka River area, located at the eastern end of the Mesabi range, is at the intersection of these three major subdivisions of the Precambrian (Fig. 1).

The Biwabik Iron Formation extends as a belt E-NE across northern Minnesota for about 120 miles. This formation has a maximum thickness of about 800 feet in the central part of the Mesabi range (White, 1954); however, it thins progressively eastward through the Eastern Mesabi district so that it is 175–300 feet thick in the Dunka River area. The iron formation is present for about 3 miles along strike in the Dunka River area. The outcrop belt strikes N-NE; it is less than one-fourth mile wide and the formation generally dips 15°–35° southeastward. Prior to mining, the iron formation in the area was mapped in detail by the writer (Bonnichsen, 1968); a generalized geologic sketch map is included in this report (Fig. 2).

The Virginia Formation in the Dunka River area is generally less than 50 feet thick, but locally is as much as 100 feet thick. In the northern part of the area it is absent so that the iron formation is in contact with the Duluth Complex. The portion of the Duluth Complex that is present in the Dunka River area is part of the South Kawishiwi Intrusion and consists predominantly of troctolite. Sills and dikes related to the Duluth Complex locally intrude the iron formation and overlying Virginia Formation.

On the basis of mineralogy and bedding characteristics, the iron formation has traditionally been subdivided into four members, from oldest to youngest: Lower Cherty, Lower Slaty, Upper Cherty, and Upper Slaty. These four members are recognized in the Dunka River area (Table 1).

Along most of the Mesabi range, the Biwabik Iron Formation consists principally of quartz, iron oxides (magnetite and hematite), carbonates (impure siderite and ankerite), and iron silicates (mainly stilpnomelane, minnesotaite, and greenalite). The rocks generally are fine-grained; all of the minerals commonly are less than 0.1 mm in maximum diameter. The iron formation displays a wide variety of bedding features, small-scale structures, and textural features such as granules and replacement textures. It is complexly layered with individual layers ranging from less than one-tenth inch, to several inches thick; this layering consists predominantly of quartz-rich material alternating with material rich in magnetite, siderite, or iron silicates that may be laminated. In addition, it is layered on larger scales by variations in overall bedding characteristics and amounts of the minerals.

In the Eastern Mesabi district where the iron formation is highly metamorphosed, the place of the carbonates and early iron silicates is taken by amphiboles, pyroxenes, fayalite and locally by garnet and other silicates. Here the small-scale pre-metamorphic textural features such as granule outlines have been partially to completely destroyed; the larger structures and complex bedding relationships have been little affected by the metamorphism, however.

Mineralogy. The iron formation in the Dunka River area consists mainly of quartz, magnetite, orthopyroxene, Ca pyroxene, fayalite, cummingtonite, and hornblende, with minor quantities of garnet (almandine and andradite), feldspar, biotite, apatite, pyrrhotite, calcite, wollastonite, iron-rich serpentine, and talc. Other minerals include chalcopyrite, molybdenite, graphite, rhodonite, manganiferous pigeonite, epidote, chlorite, and xanthopyllite or clintonite; also, cordierite occurs in the Virginia Formation. The stratigraphic distribution of the principal minerals and some of the less abundant ones is shown in Figure 3.

Quartz is the most abundant mineral in the iron formation and occurs in all stratigraphic units of the formation. Most is localized in quartz-rich laminae and thin beds. The present distribution of quartz is approximately the same as it was prior to metamorphism; locally, however, it was consumed by reaction with the original carbonates, resulting in quartz-free laminae and thin beds that are rich in pyroxenes or fayalite.

Magnetite is second in abundance to quartz in the iron formation. Its distribution and abundance is essentially the same as prior to metamorphism. Where ferrohypersthene is abundant, much of the magnetite is fine-grained and poikilitically enclosed in large ferrohypersthene grains.

Nomenclature. The following nomenclature has been adopted in this report for amphiboles, pyroxenes, and olivine.

The name cummingtonite is used for all monoclinic Ca-poor amphiboles of the cummingtonite-grunerite series even though the atomic Fe/(Mg+Fe) ratio of a few is greater than 70 percent and they would be referred to as grunerite by some authors.

The name hornblende is used for Ca amphiboles regardless of their Al_2O_3 content rather than referring to the few with low Al_2O_3 contents as actinolite. Those with abundant Al_2O_3

and those deficient in Al_2O_3 look alike in thin section. The range of Al_2O_3 encountered is 2.4 to 10.2 weight percent and there is a continuous gradation between these values.

Orthorhombic Ca-poor pyroxenes with atomic Fe/(Mg+Fe) ratios of less than 50 percent are referred to as hypersthenes and those with ratios greater than 50 percent are referred to as ferrohypersthenes.

Calcium pyroxenes with atomic Fe/(Mg+Fe) ratios less than 50 percent are referred to as diopsides and those with ratios over 50 percent are called hedenbergites. Some writers would use the term ferroaugite for many of the hedenbergites because of their deficiency in Ca with respect to Mg plus Fe from the ideal formula of $Ca(Fe,Mg)Si_2O_6$.

The olivines generally are referred to as fayalites and most have atomic Fe/(Mg+Fe) ratios of 90 percent or slightly more.

Mineral assemblages. Quartz, magnetite and orthopyroxene is the basic mineral assemblage in most parts of the iron formation in the Dunka River area. The Fe/(Mg+Fe) ratio of orthopyroxene varies considerably in different parts of the formation. Fayalite is present in rocks that have high Fe/(Mg+Fe) ratios. In rocks that contain fayalite but lack quartz, the fayalite commonly has a lower Fe/(Mg+Fe) ratio than in rocks which contain quartz. If sufficient Ca is available, Ca pyroxene is present. The development of cummingtonite indicates the presence of H_2O, but the mineral commonly is paragenetically later than associated pyroxenes or fayalite. The occurrence of hornblende, which generally is later than associated pyroxenes, indicates the presence of Al.

The four solid solution minerals, orthopyroxene, Ca pyroxene, cummingtonite, and hornblende, commonly accompanied by quartz and magnetite, coexist through a wide range of Fe/(Mg+Fe) ratios, fayalite also may be present. When all of these minerals occur together their compositions have fixed values. If quartz is absent, it is possible for two pyroxenes, two amphiboles, and olivine to coexist through a range of Fe/(Mg+Fe) ratios richer in Mg than if in the presence of quartz.

Nature and conditions of metamorphism. The iron formation is believed to have been essentially unmetamorphosed prior to the intrusion of the Duluth Complex. From measurements of oxygen isotope ratios in coexisting quartz and magnetite from various localities along the Mesabi range, Perry and Morse (1967) estimate that the maximum temperature attained in the part of the formation unaffected by the Duluth Complex may be as low as 100°C or less.

During intrusion of the Duluth Complex the thermal history of the iron formation in the Dunka River area evidently consisted of a rapid temperature increase followed by a temperature maximum and a comparatively long time during which the thick overlying mass of mafic magma crystallized and cooled. The O^{18}/O^{16} ratios of quartz and magnetite from several Dunka River area samples were determined for the writer by E. C. Perry, Jr. and are reported by Perry and Bonnichsen (1966). The O^{18}/O^{16} ratios were converted to estimated temperatures by utilizing the quartz-magnetite "geothermometer" developed by O'Neil and Clayton (1964). The maximum temperature attained at the intrusive contact and in the upper part of the iron formation is estimated to be between 700° and 750°C. The temperature maximum probably was slightly less at the base of the iron formation (300 to 400 feet from the intrusive contact).

The metamorphism of the iron formation is believed to have been isochemical except for the loss of CO_2 and most of the original H_2O.

The sequence of mineralogic reactions that occurred in the iron formation during prograde metamorphism and the subsequent prolonged retrograde metamorphism are readily apparent in the textural relationships among the various minerals. The writer has attempted to distinguish two general categories of textures: (1) Minerals which are approximately contemporaneous (and probably in mutual equilibrium) that formed during prograde metamorphism are referred to as early minerals. (2) Minerals formed during retrograde metamorphism which are later than associated minerals are referred to as late minerals. Prograde metamorphism consisted mainly of the

TABLE 1. SUMMARY DESCRIPTIONS OF STRATIGRAPHIC UNITS WITHIN THE BIWABIK IRON FORMATION IN THE DUNKA RIVER AREA

Member

Upper Slaty

(25–85 feet thick)

Upper part: interlayered quartz and Ca pyroxene at base; heterogeneous assortment of marble, calc-silicate rock, and hornfels at top; contains almost no magnetite.

Lower part: laminated orthopyroxene-magnetite-quartz taconite containing lenticular quartz-rich beds and local slump structures at base; much fine-grained magnetite enclosed in large orthopyroxenes; grades upward to laminated fayalite-rich ferrohypersthene-magnetite-quartz taconite containing local pyrrhotite and graphite, interlayered with quartz-rich beds; serpentine-magnetite veinlets parallel to layering in fayalite-rich beds impart banding; diabase sill located near top of unit.

Upper Cherty

Upper part: (20–40 feet thick) quartz-magnetite-hedenbergite taconite having variable bedding but characterized by a few thin beds with half-inch hedenbergite mottles at base; grades upward into laminated orthopyroxene-magnetite-quartz taconite interlayered with quartz-rich beds; much fine-grained magnetite enclosed in large orthopyroxenes.

Middle part: (30–45 feet thick) wavy-layered to conglomeratic quartz-magnetite taconite containing pyroxenes and amphiboles; lacks fayalite; silicates more abundant toward base, magnetite increases upward; wavy magnetite layers have sharp contacts, much is medium-grained.

Lower part: (20–45 feet thick) even-bedded quartz-magnetite-ferrohypersthene-fayalite taconite at base; grades upward into wavy-layered quartz-magnetite taconite containing abundant ferrohypersthene, hedenbergite, and fayalite; hedenbergite-pegmatites locally are present along layering; magnetite layers have fairly sharp borders, much is medium-grained.

Lower Slaty

(50–70 feet thick)

Upper part: indistinctly-layered ferrohypersthene-quartz-fayalite-magnetite taconite; fayalite is absent locally; magnetite mainly in irregular very thin magnetite-rich beds.

Lower part: nearly massive fayalite-ferrohypersthene taconite containing local pyrrhotite and almandine garnet; generally contains quartz; virtually no magnetite; serpentine-magnetite veinlets parallel to layering in fayalite taconite impart banding; presumably equivalent to Intermediate Slate.

Lower Cherty

(0–35 feet thick)

Heterogeneous assortment of quartz-rich, ferrohypersthene-magnetite, and hedenbergite-rich taconite; local feldspathic beds resemble Pokegama Quartzite; Mn silicates are locally present.

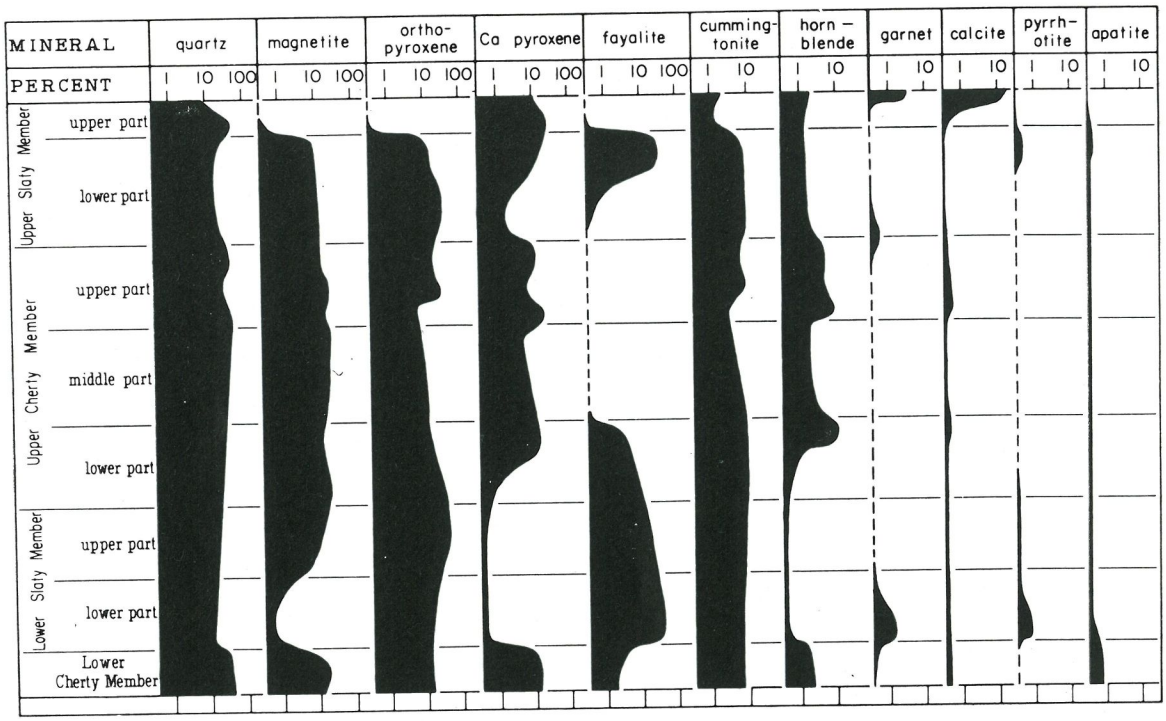

FIG. 3. Abundance of various minerals in the Biwabik Iron Formation in the Dunka River area.

development of anhydrous pyroxenes and fayalite from the original carbonates and phyllosilicates. The retrograde reactions consisted principally of the development of amphiboles from pyroxenes and fayalite and complex exsolution phenomena in the pyroxenes.

Mineral analyses. Partial chemical analyses of pyroxenes, fayalites and amphiboles from 26 taconite samples are tabulated in this report. These analyses were made by the writer using the Materials Analysis Corporation Model 400 electron microprobe located at the Department of Geology and Geophysics, University of Minnesota. In addition, two mineral separates that are reported were analyzed by conventional wet chemical means in the U.S. Geological Survey laboratories; these are a hedenbergite (sample 330) and a hornblende (sample 262).

Previously analyzed orthopyroxenes, Ca pyroxenes, olivines, and hornblendes were used as standards for quantitative analysis of the various silicates. The cummingtonite analyses were made using orthopyroxenes for standards.

It was assumed that all of the iron is ferrous in both standards and unknowns; consequently, FeO represents total iron reported as FeO. In general, the analyses for MgO, FeO and CaO were found to be reproducible to somewhat better than 5 percent; some minerals, however, commonly have greater compositional ranges than this, especially Ca pyroxenes and cummingtonites. Reproducibility data was not obtained for MnO or Al_2O_3; however, the analyses for these oxides are considered to be as reproducible as those for MgO, FeO, and CaO. Part of the SiO_2 analyses may be somewhat inferior to those for the other oxides; the SiO_2 calibration curves were constructed by using samples from the different mineral groups in order to span significant ranges of SiO_2 percentage. A greater amount of scatter was present in these SiO_2 calibration curves than in the calibration curves for the other oxides.

In most rocks the MgO, FeO, and CaO percentages were determined for all the silicate minerals during the same microprobe run so the results would be more precise relative to one another than if they were determined at different times. By this means the effects of instrumental fluctuations and calibration curve errors, which are the causes of the reproducibility error, are believed to have been partially eliminated.

An indication of the completeness and accuracy of a chemical analysis is how near the sum of its constituents approaches 100 percent. The percentages of the major oxides (MgO, FeO, CaO, MnO, Al_2O_3, and SiO_2) were measured in 46 of the fayalite, pyroxene, and amphibole analyses reported here. For more than half of these analyses the sum of the major oxides is within 1 percent of 100 percent (98% for amphiboles) and 70 percent of the sums are within 2 percent.

In some minerals the concentration of certain elements is sufficiently low so that only background values of radiation were detected; in such cases, the abbreviation "b.v." has been reported.

PYROXENES AND FAYALITE

Orthopyroxene. Orthopyroxene is present throughout the iron formation and is the most abundant ferromagnesian silicate in the formation; nearly all is ferrohypersthene and a significant amount has inverted from pigeonite. The orthopyroxenes that are inverted from pigeonite are indicated by the configuration of the Ca pyroxene exsolution lamellae which they contain.

Orthopyroxene grains characteristically are disproportionately large in comparison to grains of associated minerals; they typically are ½ to 2 cm across in areas where abundant and locally are more than 5 cm across. These large crystals commonly are flattened parallel to the layering and generally contain numerous inclusions of magne-

TABLE 2. COMPOSITIONS OF ORTHOPYROXENES AND PIGEONITES

Sample Number	Wt %							Atomic Proportions	
	MgO	FeO	CaO	MnO	Al_2O_3	SiO_2	Total	Mg / Mg+Fe+Ca	Fe / Mg+Fe+Ca
006 (a)[a]	7.2	41.2	1.2	—	—	—	49.6	0.231	0.741
(b)[b]	7.3	38.6	3.1	—	—	—	49.0	.234	.694
026	8.1	40.2	0.9	0.6	0.5	50.0	100.3	.259	.721
073	11.5	35.0	1.3	—	—	—	47.8	.359	.612
082	7.0	42.0	0.8	0.6	—	49.5	99.9	.225	.757
087	7.5	41.0	0.3	1.7	—	49.5	100.0	.244	.749
088	12.0	37.5	0.2	1.1	1.8	—	52.6	.362	.634
122[a]	6.5	42.7	1.4	0.4	b.v.	51.1	102.1	.207	.761
131	25.0	20.0	0.5	0.2	0.7	55.5	101.9	.683	.307
140	14.0	31.5	1.2	3.3	b.v.	52.5	102.5	.430	.543
142 (a)[a]	8.4	37.1	1.4	3.6	0.4	—	50.9	.278	.689
(b)[b]	8.7	35.3	3.2	3.1	0.4	—	50.7	.282	.643
175	7.5	40.0	0.5	—	—	—	48.0	.247	.741
208 (a)[a]	8.1	36.0	1.2	—	—	—	45.3	.278	.693
(b)[b]	8.2	34.0	3.2	—	—	—	45.4	.277	.645
219[c]	2.5	31.5	4.5	13.0	b.v.	49.0	100.5	.107	.755
234	6.2	41.8	1.1	2.2	b.v.	50.4	101.7	.204	.770
241[d]	8.0	37.0	1.4	3.3	b.v.	50.0	99.7	.269	.697
266	11.0	34.0	1.4	3.4	b.v.	50.1	99.9	.354	.614
304	20.5	26.0	1.0	0.7	0.5	53.2	101.9	.572	.408

[a] Ferrohypersthene inverted from pigeonite.
[b] Approximate pigeonite composition.
[c] Uninverted manganiferous pigeonite.
[d] Late ferrohypersthene in incipient pegmatite.

tite; they also commonly contain inclusions of quartz, fayalite, or hedenbergite. Where orthopyroxene is a minor constituent, however, the grains ordinarily are small and not poikilitic.

Some rocks contain numerous small orthopyroxene grains, and in local areas, all the grains have nearly parallel crystallographic orientations. These sets of small, nearly parallel grains evidently formed by the breaking apart of much larger grains; locally, these areas of nearly parallel grains define relict euhedral outlines. The reason for the breaking apart of these large ferrohypersthene crystals is not known.

Orthopyroxene and fayalite occur together throughout much of the iron formation. Where fayalite is abundant the grains of both minerals generally are about the same size; where ferrohypersthene is abundant and fayalite minor, however, fayalite grains commonly are enclosed in the ferrohypersthene, and many have been partly replaced. Ferrohypersthene occurs as partial rims between quartz and fayalite grains in some rocks. Compositional differences between individual grains and the partial rims of orthopyroxene were not detected; equilibrium evidently was attained after these textures were produced.

Late-stage euhedral orthopyroxenes, associated with coarse-grained hornblende and quartz, are locally present in pegmatitic patches. In sample 241 in which this feature was studied, the orthopyroxene in the enclosing rock is inverted pigeonite, whereas the later euhedral ferrohypersthene crystallized initially as orthopyroxene and is contemporaneous with coarse-grained hornblende. The composition of this late ferrohypersthene is within the compositional range of pigeonite; presumably, it crystallized at a temperature lower than the pigeonite-ferrohypersthene inversion temperature.

The compositions of orthopyroxenes from several rocks were determined (Table 2); their Fe/(Mg+Fe) percentages are plotted against their Ca/(Mg+Fe+Ca) percentages in Figure 4. The compositions of coexisting cummingtonites that are believed to be in approximate equilibrium with the orthopyroxenes also are plotted. The average Fe/(Mg+Fe) ratio for the six orthopyroxenes plotted in Figure 4 that occur with quartz and fayalite is 76.7 percent.

Prior to inversion, the pigeonites contained approximately 3.0–3.5 weight percent CaO; this corresponds to 7.0–8.0 atom percent Ca/(Mg+Fe+Ca). The inverted pigeonites whose compositions were measured contain more than 71 percent Fe/(Mg+Fe) (69% for pre-inversion ratio).

Manganiferous pigeonite. An interesting Mn-rich pyroxene was found in a quartz-rich sample (219) from the lowermost part of the iron formation. The mineral evidently is a manganiferous pigeonite which has not inverted to an orthorhombic structure; it is yellowish-tan in hand sample and localized along irregular laminae within the quartz-rich matrix. Its composition is given in Table 2. It contains 4.5

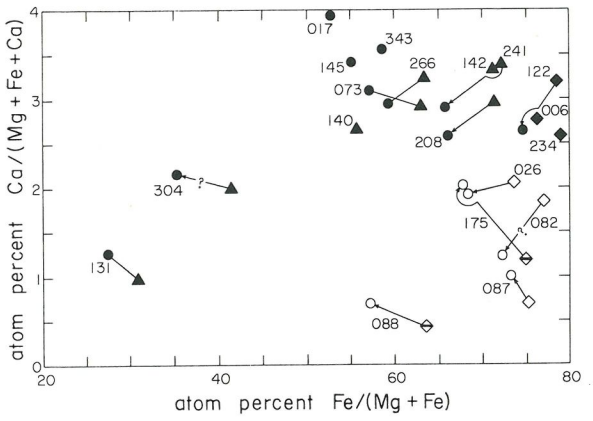

Orthopyroxenes

◆ ◇ fayalite and quartz present

▲ fayalite absent

◈ fayalite present, quartz absent

Cummingtonite: contemporaneous with orthopyroxene or prismatic replacement of orthopyroxene, and in rocks which lack

● ○ orthopyroxene

Filled symbols: Ca pyroxene or early hornblende present

Open symbols: Ca pyroxene and early hornblende absent

——— contemporaneous or ambiguous time relationship

←——— cummingtonite is later than and may replace orthopyroxene

FIG. 4. Compositions of orthopyroxenes and cummingtonites from the Dunka River area. Orthopyroxenes 006, 122, 142 and 208 are inverted from pigeonite.

percent CaO like ordinary igneous pigeonites but contains only 2.5 percent MgO, much lower than other pyroxenes. Its atomic Mn/(Mg+Fe+Mn) ratio is 26.8 percent and it is replaced by small prismatic cummingtonite grains that contain 15.3 percent Mn/(Mg+Fe+Mn). In thin section it is very light yellow (almost colorless) and non-pleochroic with a birefringence of approximately 0.012. It has inclined extinction, a biaxial positive figure with a low 2V, and the optic plane is perpendicular to (010).

Calcium pyroxene. Calcium pyroxene is abundant in certain stratigraphic intervals of the iron formation but is virtually absent from others (Fig. 3). Most of the Ca pyroxene is hedenbergite, although locally it has a composition that is intermediate between hedenbergite and diopside and in the upper part of the formation most is diopside.

The grains commonly are coarse- or medium-sized and quite irregular; they have interlocking boundaries in textural units that consist principally of hedenbergite. In layers of fine-grained Ca pyroxene, however, the grains are equidimensional and commonly occur in an equigranular mosaic texture. Calcium pyroxene in quartz-rich layers generally is fine-grained and anhedral if it is disseminated; in those rocks it commonly is closely associated with orthopyroxene and partly replaced by hornblende.

Calcium pyroxene commonly encloses small amounts of magnetite but only in a few rocks was Ca pyroxene observed to contain abundant magnetite inclusions in the same manner as ferrohypersthene. Calcium pyroxene grains are not common as inclusions in other minerals except as exsolution lamallae and blebs in orthopyroxene.

Very Fe-rich hedenbergites form distinctive thin beds in the vicinity of the Upper Cherty-Upper Slaty contact. These strongly pleochroic Fe-rich hedenbergites commonly are partly replaced by much more diopsidic non-pleochroic Ca pyroxene, especially adjacent to quartz-rich laminae. An interesting, but restricted, occurrence of these Fe-rich hedenbergites is as very early-formed inclusions within quartz and andradite garnet grains. In the same rock in which these inclusions were noted (134), larger later-formed Ca pyroxene grains with intermediate compositions are present and are approximately contemporaneous with andradite garnet.

Exsolution lamellae of Ca-poor pyroxene parallel to (001) are present in most Ca pyroxenes which coexist with cummingtonite or orthopyroxene. Exsolution lamellae of Ca-poor pyroxene that parallel the (100) plane of Ca pyroxenes are rare, however.

Throughout much of the iron formation the Ca pyroxene grains are riddled with very fine-grained alteration patches. The altering material generally is too fine-grained to identify with any certainty, but where sufficiently coarse it is seen to be either cummingtonite or hornblende. It is common for adjacent patches of altering amphibole to be crystallographically parallel. In a few Ca pyroxenes, the altering amphiboles have formed along definite crystallographic planes. Much of the replacement of Ca pyroxene by hornblende occurs at the margins of grains; where strongly developed, however, patches of hornblende also occur inside of the Ca pyroxene grains. The replacement of Ca pyroxene by cummingtonite virtually is confined to internal alteration patches.

A number of Ca pyroxenes were analyzed (Table 3); their atomic proportions of Mg, Fe, and Ca are plotted in Figure 5. In this figure it can be seen that Ca pyroxenes from rocks containing Ca-poor pyroxene or cummingtonite are generally richer in Mg than those from rocks lacking orthopyroxene and cummingtonite.

Considerable compositional variation within individual grains is a characteristic of most of the Ca pyroxenes. The weight percent of CaO and FeO generally varies by 2 or 3 percent; the variation for MgO usually is much smaller, however. Much of this variation is believed to be due to very fine-grained and subvisual unmixing.

Calcium pyroxenes whose margins are strongly replaced by hornblende show the largest compositional shifts; the amount of this was measured, although not too accurately, in samples 145 and 149 as indicated in Figure 5. The principal change accompanying the alteration was loss of Fe with respect to Ca. With the very fine-grained alteration by probable cummingtonite, however, there is little detectable shift in pyroxene compositions.

Fayalite. Fayalite is present in parts of the iron formation; locally it is the most abundant mineral, particularly in the Lower Slaty Member. It is absent from the other parts of the formation, generally where hedenbergite is an important mineral (Fig. 3). This is believed to indicate differences in the original carbonates of the iron formation; the fayalite having formed mainly from siderite whereas hedenbergite formed from ankerite.

Most fayalite grains are anhedral, approximately equidimensional, one millimeter or less in diameter, and uniform in size within a textural unit. Larger fayalite grains are present locally; these grains commonly contain quartz and magnetite inclusions. Fayalite grains commonly occur together in clusters or are concentrated in layers; the mineral nearly always is accompanied by ferrohypersthene and cummingtonite, and generally by quartz and magnetite. Locally, fayalite occurs in quartz-free nearly monomineralic beds as much as several inches thick.

Fayalites from a number of rocks were analyzed; their compositions are listed in Table 4. The fayalite compositions from rocks containing quartz are essentially identical and average 90.7 atom percent Fe/(Mg+Fe). Fayalites from rocks which lack quartz are variable in composition; all contain more Mg than those with quartz.

Coexisting pyroxenes and fayalite. Coexisting pyroxenes from several rocks were analyzed; their compositions are plotted in Figure 6. The pre-inversion pigeonite compositions of samples 006, 142, and 208 and the fayalite compositions also are plotted. These minerals are believed to have crystallized contemporaneously between 700° and 750° C., with the exception of the ferrohypersthene in sample 241. It occurs with coarse-grained hornblende in an incipient pegmatite that is texturally later than associated hedenbergite and inverted pigeonite and most likely formed at a slightly lower temperature.

TABLE 3. COMPOSITIONS OF CA PYROXENES

Sample Number	Wt %							Atomic Proportions		Comments
	MgO	FeO	CaO	MnO	Al_2O_3	SiO_2	Total	Mg / Mg+Fe+Ca	Fe / Mg+Fe+Ca	
006	6.5	22.0	20.5	—	—	—	48.0	0.193	0.368	
017	10.0	17.0	20.0	—	—	—	47.0	.295	.281	Weakly altered[a]
073	9.0	18.5	19.0	—	—	—	46.5	.272	.314	Moderately to strongly altered
119	10.0	13.5	26.0	—	—	—	49.5	.276	.209	
122	6.1	23.0	20.0	0.2	0.7	53.1	103.1	.183	.386	
134 (a)	2.9	26.0	24.5	1.4	1.7	—	56.5	.082	.416	Early relicts in quartz and andradite
(b)	9.9	13.7	26.9	1.6	0.8	—	52.9	.268	.208	Approximately contemporaneous with andradite
135	3.0	22.75	21.75	1.0	—	—	48.5	.096	.406	Locally replaced by more diopsidic Ca pyroxene
140	11.0	16.0	20.0	1.9	b.v.	51.0	99.9	.320	.261	Moderately to strongly altered
142	7.8	20.5	19.4	1.8	0.9	—	50.4	.235	.346	
145 (a)	10.5	15.9	19.0	—	—	—	45.4	.317	.270	Approximate pre-alteration composition
(b)	10.4	14.7	20.3	—	—	—	45.4	.313	.248	Moderately to strongly altered grains
149 (a)	5.5	19.5	20.5	1.8	b.v.	—	47.5	.176	.351	Average composition
(b)	5.1	21.0	19.7	—	—	—	45.8	.164	.380	Unaltered areas
(c)	5.9	18.0	22.0	—	—	—	45.9	.185	.318	Strongly altered areas
173	5.5	20.5	21.0	1.2	b.v.	—	48.2	.171	.358	Strongly altered
208	8.3	19.8	19.3	—	—	—	47.4	.249	.334	Poor analysis
210	6.7	18.4	23.5	—	—	—	48.6	.198	.304	Strongly altered
241	7.5	19.0	20.5	1.8	0.5	48.0	97.3	.228	.324	Strongly altered
266	9.0	17.5	20.0	1.5	b.v.	52.4	100.4	.271	.296	Unaltered to moderately aleterd
304	13.5	10.5	22.0	0.3	0.7	53.0	100.0	.384	.167	Weakly altered
330[b]	3.50	22.88	21.02	2.30	0.81	49.20	100.67	.111	.408	Wet chemical analysis
343	10.0	17.0	20.0	1.0	0.3	52.0	100.3	.295	.281	Srotngly altered

[a] The alteration of Ca pyroxene consists of numerous alteration patches disseminated throughout grains, most of which are too fine to be identified. Locally, where sufficiently coarse-grained they are seen to be cummingtonite or hornblende.

[b] FeO consists of 21.53 percent FeO and 1.50 percent Fe_2O_3 reported as FeO; the total includes 0.28 percent Na_2O, 0.25 H_2O+, 0.10 H_2O-, 0.06 P_2O_5, 0.05 CO_2 and 0.07 C exclusive of CO_2. The analysis indicates that less than 0.0005 K_2O, 0.00 TiO_2 and less than 0.01 S are present. (L. E. Reichen, analyst).

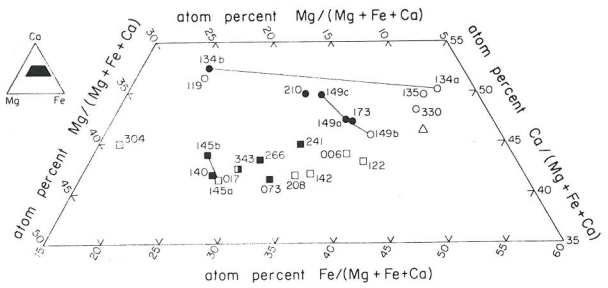

□ ■ Orthopyroxene or cummingtonite present. (The Ca pyroxenes in samples 017 and 343 coexist with cummingtonite only.)

○ ● Orthopyroxene and cummingtonite absent.

△ Hedenbergite reported by Gundersen and Schwartz (1962).

Open symbols—unaltered pyroxenes.
Filled symbols—significant alteration or replacement by hornblende.

FIG. 5. Compositions of Ca pyroxenes from the Eastern Mesabi district. The Ca pyroxenes in samples 006, 119, and 122 coexist with olivine and those in 006, 122, 142 and 208 coexist with inverted pigeonites.

Equilibrium phase relationships. Figure 7 is an isothermal section showing the phase relationships proposed to hold among the pyroxenes and fayalite plus quartz at the maximum temperature and other metamorphic conditions achieved in the Dunka River area. The dash-dot-dot line is drawn through the compositions of Ca pyroxenes that coexist with Ca-poor pyroxenes in the Skaergaard intrusion as reported by Brown (1957). This is the best available estimate of the boundary position between the Ca pyroxene field and the two-pyroxene field at magmatic temperatures. Note the shift in position of this boundary from magmatic temperatures to the metamorphic temperatures attained in the Dunka River area.

Figure 8 is a temperature-composition plot from the Ca-poor side to the Ca-rich side of the pyroxene quadrilateral that shows the phase relations proposed among iron-rich Ca pyroxene, pigeonite, and orthopyroxene. The manner in which this figure is drawn is similar to figures published by Poldervaart and Hess (1951), Muir (1954), and Kuno (1966).

Recently, Dallwitz, Green, and Thompson (1966) analyzed clinoenstatite crystals contained in a volcanic rock from eastern New Guinea, which they interpret to have inverted from original protoenstatite phenocrysts. These clinoenstatite crystals are associated with primary orthopyroxene crystals. Utilizing their information, and some possible phase relationships proposed by Boyd and Schairer (1964), Dallwitz, Green, and Thompson proposed the phase relationships shown on the Mg-rich side of Figure 9 for protoenstatite, pigeonite, and orthopyroxene. Combining these relationships with the phase relationships proposed in Figures 7 and 8, the iron-rich side of Figure 9 has been constructed; this figure indicates the subsolidus phase relationships proposed to hold among Ca-poor pyroxenes and fayalite plus quartz for all Fe/(Mg+Fe) ratios at pressures obtained within a few miles of the Earth's surface. This figure is similar to one published by Kuno (1966); his estimate of the pigeonite-orthopyroxene inversion temperature for iron-rich compositions is much higher, however. It is important to note that Figure 9 depicts relationships along the irregular-shaped surface of Ca-poor pyroxene that coexists with Ca pyroxene within the temperature-composition volume, rather than along the En-Fs sideline.

Exsolution and inversion in pyroxenes. Well-developed exsolution lamellae are present in most of the coexisting pyroxenes from the Dunka River area. Two sets of lamellae are associated with orthopyroxene. The earlier set was developed along (001) of former pigeonite grains and are enclosed in orthopyroxene grains at random orientations. The later set is developed along (100), parallel to the optic plane of the orthopyroxene grains (Fig. 10). In Ca pyroxene, nearly all exsolution lamellae are developed along (001); lamellae parallel to (100) are rare and very thin.

TABLE 4. COMPOSITIONS OF OLIVINES

Sample Number	Wt %							Atomic Proportion Fe / Mg+Fe
	MgO	FeO	CaO	MnO	Al_2O_3	SiO_2	Total	
006	3.5	65.5	0.1	—	—	—	69.1	0.913
026	4.0	67.5	—	—	—	32.0	103.5	.904
082	3.5	65.5	b.v.	0.6	—	33.0	102.6	.913
087	4.0	64.0	b.v.	1.8	—	33.0	102.8	.900
088	7.0	62.0	0.1	1.1	b.v.	—	70.2	.833
119	11.5	53.5	0.2	—	—	—	65.2	.723
122	3.4	62.7	—	0.5	b.v.	32.9	99.5	.912
175	4.5	62.0	0.2	—	—	—	66.7	.885
234	3.8	61.7	—	2.4	b.v.	32.9	100.8	.901

Quartz is present in samples 006, 026, 082, 087, 122 and 234.
Quartz is absent in samples 088, 119 and 175.

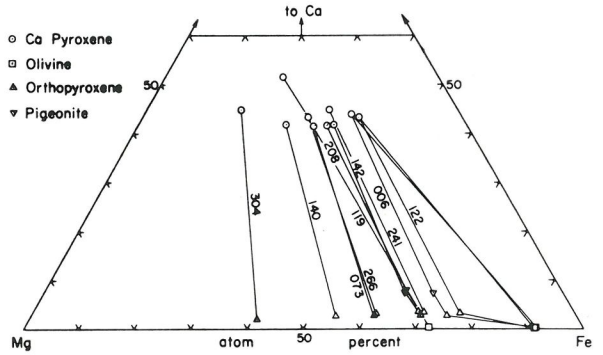

FIG. 6. Orthopyroxenes and olivines coexisting with Ca pyroxenes. Also shown are the initial compositions for the inverted pigeonites in samples 006, 142 and 208. Orthopyroxene is not present in sample 119 and quartz is not present in samples 119 and 142.

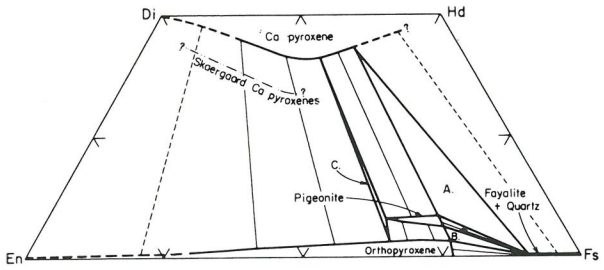

FIG. 7. Equilibrium phase relationships proposed to hold among coexisting pyroxenes and fayalite plus quartz at the maximum temperature (700°–750°C) and other conditions attained during metamorphism of the Biwabik Iron Formation in the Dunka River area. A.—Ca pyroxene, pigeonite, and fayalite plus quartz; B.—pigeonite, orthopyroxene, and fayalite plus quartz; C.—Ca pyroxene, pigeonite, and orthopyroxene. The dash-dot-dot line represents the compositions of Skaergaard Ca pyroxenes which coexist with Ca-poor pyroxenes (Brown, 1957). An alternate relationship, also consistent with the available information, would be for the pigeonite field to be expanded farther toward the Fs corner so that it would intersect the En-Fs sideline between the fayalite plus quartz and orthopyroxene fields.

Lamellae in orthopyroxene. In ferrohypersthene grains that contain well-developed relict (001) Ca pyroxene lamellae, domains of these lamellae outline the boundaries between the pre-existing pigeonite grains (Figs. 11 and 12). The initial pigeonite grains were about the same size as contemporaneous fayalite and hedenbergite grains. Where abundant, the pigeonites had formed an equigranular mosaic texture, similar to that commonly found among fayalite grains and in some laminae rich in hedenbergite. There is no correspondence between the boundaries of pre-existing pigeonite grains and the present boundaries of ferrohypersthene grains (Figs. 11 and 13); also, the ferrohypersthene grains are much larger than the former pigeonite grains. The idealized sequence of changes that a group of pigeonite grains have undergone during cooling is illustrated in Figure 14.

It is indicated in Figure 14 that Ca pyroxene lamellae had begun to form along (001) in the pigeonite grains before the inversion. During the inversion, it is likely that the Ca in excess of that which could be accommodated in orthopyroxene migrated to these lamellae and formed additional Ca pyroxene, thus increasing their thickness. In other rocks, however, where the amount of Ca was only sufficient to form pigeonite these (001) lamellae did not develop before the inversion. In these cases, the Ca pyroxene liberated during the inversion occurs mainly as irregular blebs in the ferrohypersthene grains.

Locally, some ferrohypersthene grains that have inverted from pigeonite contain very fine-grained myrmekite-like intergrowths of Ca pyroxene. In other areas the unmixing between orthopyroxene and Ca pyroxene evidently has been subvisual in scale, as electron microprobe analysis in certain areas of some ferrohypersthene grains indicated high

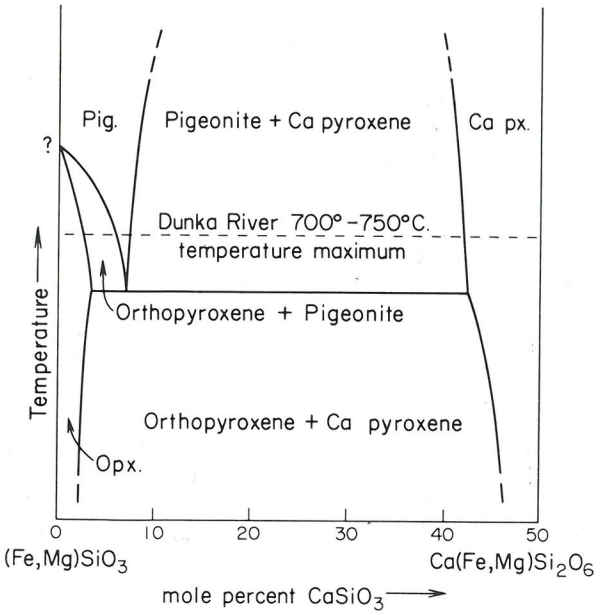

FIG. 8. Proposed temperature-composition relationships among iron-rich Ca pyroxene, pigeonite, and orthopyroxene. This figure is a section across the pyroxene quadrilateral through the fields of Ca pyroxene, pigeonite, and orthopyroxene approximately along the tie line in the Ca pyroxene-pigeonite field of Figure 7.

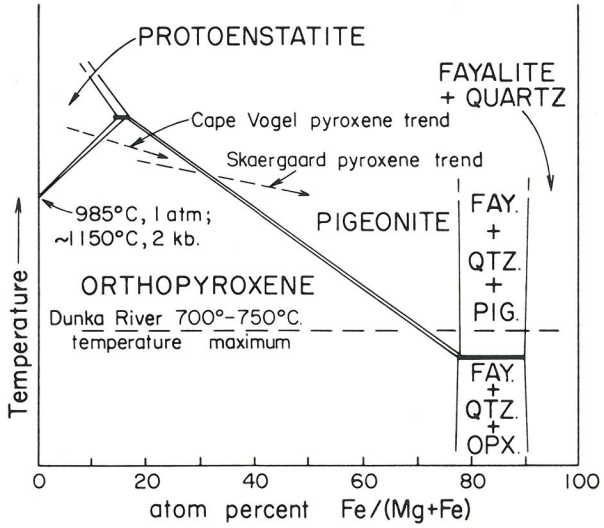

FIG. 9. Equilibrium relationships proposed to exist between protoenstatite, orthopyroxene, pigeonite, and fayalite plus quartz coexisting with Ca pyroxene for relatively low-pressure geologic situations (within a few miles of the Earth's surface). The Cape Vogel pyroxene trend (Dallwitz, Green, and Thompson, 1966) is not necessarily at a higher temperature than the Skaergaard trend (Brown, 1957), but at a lower pressure. The orthorhombic enstatite-protoenstatite inversion temperatures and proposed relationship between protoenstatite, orthopyroxene, and pigeonite are based on experiments reported by Boyd and Schairer (1964).

FIG. 10. Ferrohypersthene grain with very thin hedenbergite exsolution lamellae developed parallel to (100). This grain crystallized initially as orthopyroxene, rather than having inverted from pigeonite. The black grains are poikilitically enclosed magnetite. (Crossed nicols, ×68).

CaO and low FeO values although Ca pyroxene lamellae are not visible. Such fine-scale unmixing may have resulted from rapid inversion, possibly after considerable supercooling.

In some rocks the (100) Ca pyroxene lamellae are not developed or are only partially developed in orthopyroxene. This is common in grains that have high Mg contents and in rocks which do not contain Ca pyroxene grains. In Fe-rich rocks containing Ca pyroxene grains, the (100) lamellae commonly are present in ferrohypersthene grains, but are absent locally. They are not present in areas of subvisual unmixing. In some parts of ferrohypersthene grains that lack the (100) lamellae, the excess Ca necessary for their development evidently has migrated to nearby grain boundaries and edges of earlier-formed Ca pyroxene lamellae and blebs. In parts of some ferrohypersthene grains the loss of (100) lamellae was accompanied by the development of irregular protuberances at the edges of earlier Ca pyroxene lamellae (Fig. 12). The destruction of (100) Ca pyroxene lamellae in ferrohypersthene grains is most common in rocks and portions of rocks that contain abundant cummingtonite. This suggests that a greater amount of H_2O was available, which facilitated diffusion and the development of larger Ca pyroxene blebs in preference to the very thin lamellae. The (100) lamellae are developed best where cummingtonite is absent.

In some orthopyroxene grains, generally where late cummingtonite is abundant, the relict (001) lamellae are present only in certain parts of these large ferrohypersthene grains, mainly the central portions. In other portions of the grains, especially peripheral areas, neither the relict (001) lamellae nor irregular Ca pyroxene blebs are present. Evidently, after these ferrohypersthene grains had formed by inversion of pigeonite, they continued to enlarge at the expense of adjacent minerals, principally fayalite and quartz.

Interestingly, Poldervaart and Hess (1951) maintain that during the inversion from pigeonite to orthopyroxene, the pigeonite (*b*) and (*c*) crystallographic axes generally are retained in the orthopyroxene. Both Brown (1957) and Bown and Gay (1960), on the other hand, found for inverted pigeonites of the Skaergaard intrusion that the crystallographic axes rarely were retained through the inversion; rather, in nearly all grains which were examined, the orthopyroxene axes are oriented randomly with respect to pigeonite axes.

In ferrohypersthenes inverted from pigeonite in the Dunka River area, the pigeonite crystallographic axes were disregarded entirely, so that orthopyroxene axes as well as grain boundaries (Fig. 13) are entirely independent of the prior atomic arrangement in pigeonite. During inversion

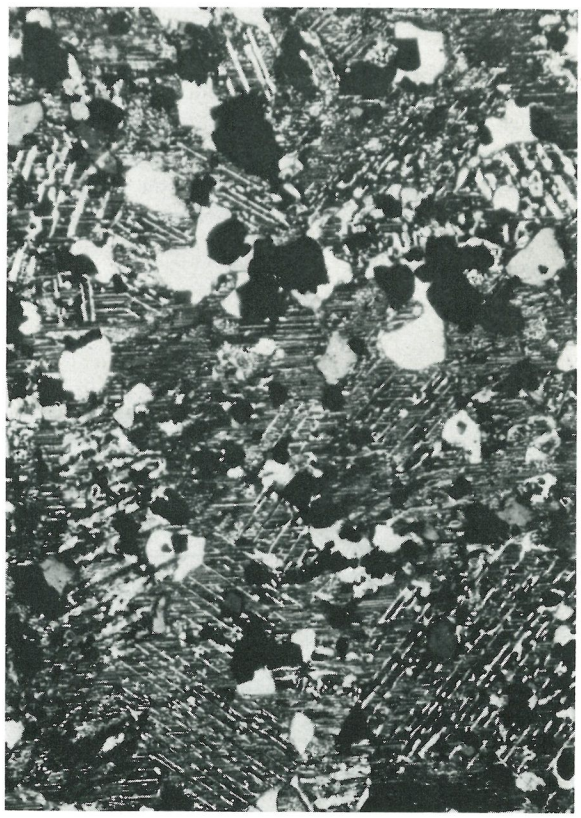

FIG. 11. A large ferrohypersthene grain that contains two sets of hedenbergite exsolution lamellae. The broader, early lamellae are segregated into domains which have diverse orientations; they formed along (001) of preexisting pigeonite grains. The lamellae which are approximately horizontal and extend entirely across the photograph developed parallel to (100) of the ferrohypersthene grain after it had inverted from the smaller pigeonite grains. The white grains are quartz and the black grains are magnetite. (Crossed nicols, ×26).

from pigeonite to orthopyroxene the crystal structure evidently was reorganized entirely, including complete reforming rather than distortion of the SiO_3 chains. As the ferrohypersthene grains are much larger than other grains with which they coexist it is evident that they were nucleated only at widely spaced points. For each ferrohypersthene grain produced by inversion of pigeonite, recrystallization must have proceeded outward from the site of nucleation as an expanding shell of crystallization along which pigeonite was breaking down, the atoms recombining into the structure of ferrohypersthene, and the excess Ca migrating to nearby Ca pyroxene lamellae or forming separate Ca pyroxene blebs in local areas.

It is possible that at the nucleation site of individual orthopyroxenes there was an initial correspondence between the orthopyroxene and pigeonite axes; however, once the growing orthopyroxene extended beyond the pigeonite in which it was nucleated, there was no longer a correspondence of old and new crystallographic axes.

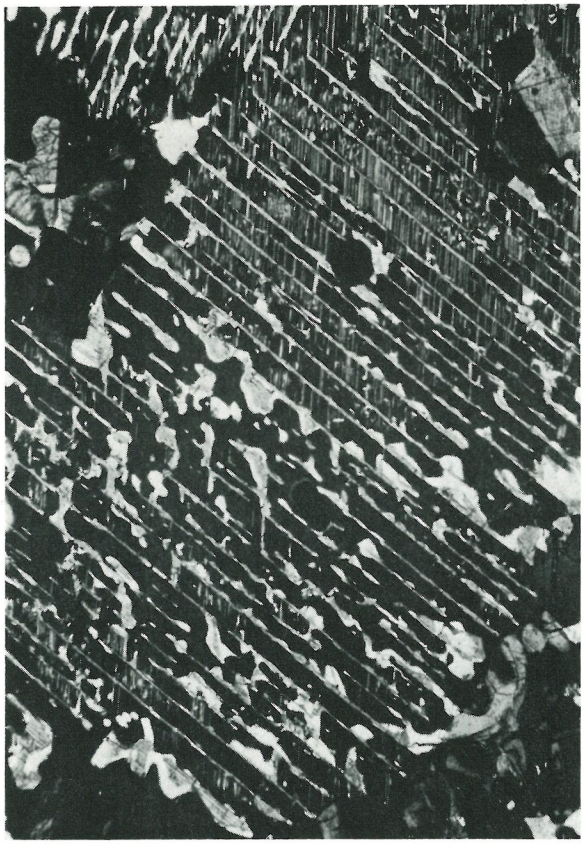

FIG. 12. A former pigeonite grain contained within a much larger ferrohypersthene grain; the outline of the pigeonite grain is delineated by the relict hedenbergite exsolution lamellae which had developed parallel to (001). The thinner, near vertical striations are hedenbergite exsolution lamellae that are parallel to (100) in the ferrohypersthene. Note that in part of the grain the later (100) lamellae are missing and in that part of the grain the (001) lamellae are characterized by conspicuous protuberances. (Crossed nicols, ×56).

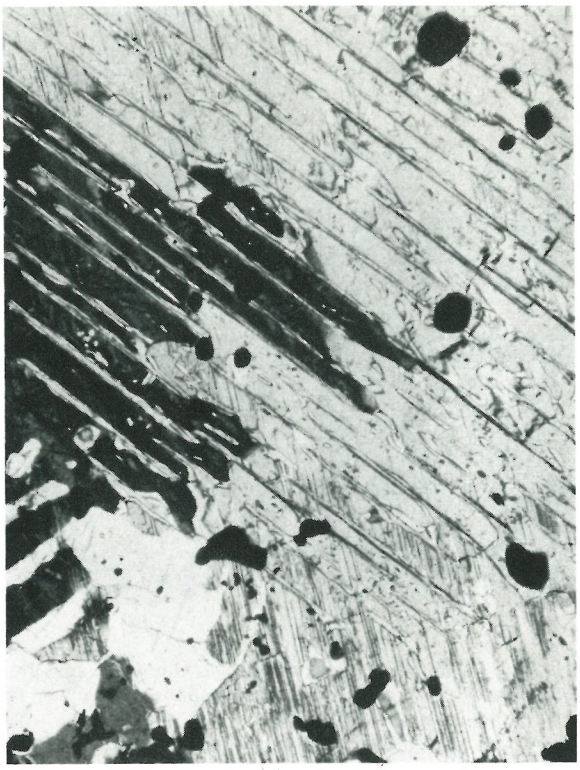

FIG. 13. Part of a former pigeonite grain in which hedenbergite exsolution lamellae had developed parallel to (001). The boundary between two adjacent ferrohypersthene grains cuts through the region occupied by the former pigeonite, disregarding the previous grain boundaries. Note that the hedenbergite lamellae extend across this grain boundary. The near vertical striations in the righthand grain are hedenbergite exsolution lamellae that are parallel to (100) of the ferrohypersthene. (Crossed nicols, ×72).

Lamellae in Ca pyroxene. Ca-poor pyroxene exsolution lamellae in Ca pyroxene grains from the Dunka River area nearly always are parallel to (001); lamellae along (100) are very thin and rare. According to Poldervaart and Hess (1951), lamellae which form parallel to (001) in Ca pyroxene are monoclinic like their host whereas pyroxene lamellae that parallel (100) are orthorhombic.

The exact nature of (001) lamellae in Ca pyroxene grains has not been resolved entirely, however. Poldervaart and Hess (1951) and others have referred to these lamellae as pigeonite because they are monoclinic. Binns, Long and Reed (1963), however, by traversing with an electron microprobe beam across thick (001) lamellae in augites from a norite from near Pretoria, South Africa, and a two-pyroxene granulite from Broken Hill, Australia, found that in these two rocks the lamellae contain only 0.7 and 0.5 weight percent CaO respectively, rather than 4 or 5 percent CaO as would be expected in pigeonite. Because of these compositions, Binns, Long, and Reed believe that these (001) lamellae belong to the clinoenstatite-clinoferrosilite pyroxene series rather than to the pigeonite pyroxene series.

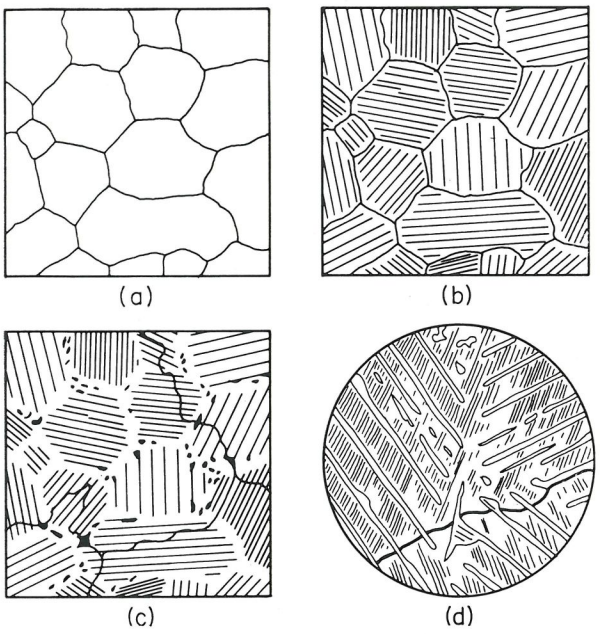

FIG. 14. Idealized sequence of changes during cooling from initial pigeonite grains to orthopyroxene grains containing two sets of Ca pyroxene lamellae.

(a) Group of approximately equidimensional pigeonite grains crystallized during prograde metamorphism.

(b) Ca pyroxene exsolution lamellae have developed along (001) during first part of cooling.

(c) After inversion of pigeonite to orthopyroxene, new orthopyroxene grain boundaries entirely disregard previous grain boundaries. Relict (001) Ca pyroxene lamellae remain, however, and define previous pigeonite grains. Irregular Ca pyroxene blebs (black spots) have formed along some of the relict (001) lamellae and in areas between former pigeonite grains.

(d) (at higher magnification) Second set of Ca pyroxene exsolution lamellae (fine lines) develop at lower temperature along (100) of orthopyroxene grains, crossing relict (001) lamellae at various angles in different areas of grains. Also possible development of (001) lamellae in local Ca pyroxene blebs after the inversion.

An attempt to determine the composition of the (001) lamellae in Ca pyroxenes from the Dunka River area was unsuccessful because all lamellae are too thin for an accurate CaO analysis. It is not known, therefore, whether the lamellae have a CaO content indicative of pigeonite or clinoferrohypersthene.

Locally, the Ca-poor (001) lamellae within Ca pyroxene grains that are adjacent to inverted pigeonites have inverted to orthopyroxene. Regardless of whether these Ca-poor (001) lamellae are pigeonite or clinoferrohypersthene, this observation indicates that the orthopyroxene crystal structure is the more stable modification, and where nucleated, the inversion of these lamellae to orthopyroxene is accomplished.

The Ca-poor (001) lamellae have formed in Ca pyroxene grains at conditions under which pigeonite grains were not stable. They are present in many Ca pyroxene grains too rich in Mg to have crystallized in equilibrium with pigeonite; furthermore, associated orthopyroxenes in such rocks do not contain the relict (001) Ca pyroxene lamellae indicative of inverted pigeonite. In some of the larger Ca pyroxene lamellae and blebs which formed during the inversion of pigeonite, there are thin (001) Ca-poor pyroxene lamellae which evidently exsolved after the inversion (Fig. 15). From these observations it is clear that the lamellae along (001) of Ca pyroxene grains are metastable with respect to orthopyroxene. It is most likely that the surrounding structure of the Ca pyroxene grains with which these lamellae share the (001) direction was influential in their development. Orthopyroxene evidently was not able to nucleate within Ca pyroxene grains and formed only if initiated by inversion from outside of enclosing Ca pyroxene grains.

Nucleation of orthopyroxene: The following observations suggest that by comparison with associated silicates, orthopyroxene was difficult to nucleate in its stability field at the temperature and other conditions prevailing in the Dunka River area, but once a crystal was initiated it was able to grow with little difficulty:

1. Orthopyroxene grains generally are disproportionately larger than coexisting silicates, whether formed initially as orthopyroxene or inverted from pigeonite.

2. Monoclinic Ca-poor pyroxene lamellae along (001) rather than orthopyroxene along (100) commonly exsolves from Ca pyroxene, even when orthopyroxene grains are present as a stable phase in the rock.

3. In some rocks Ca-poor (001) lamellae in Ca pyroxene grains have inverted to orthopyroxene and are optically parallel to the orthopyroxene grain adjacent to the enclosing Ca pyroxene grain. Presumably, these inverted lamellae were physically in contact with the adjacent pigeonite grain at the time of inversion.

4. The pigeonite crystallographic axes and grain boundaries were entirely disregarded during the inversion to orthopyroxene.

A comparatively high nucleation energy at the temperature of metamorphism is the probable reason that orthopyroxene has developed as large poikilitic grains. Orthopyroxenes that have lower Fe/(Mg+Fe) ratios are not as coarse-grained as those that have higher Fe/(Mg+Fe) ratios; this suggests the nucleation energy required to initiate an orthopyroxene grain increases with an increasing Fe/(Mg+Fe) ratio.

Some of the orthopyroxenes from the Dunka River area contain several percent of Mn. The effect of this on the pigeonite-orthopyroxene inversion temperature and the nucleation energy required for orthopyroxene is not known. The occurrence of uninverted maganiferous pigeonite in sample 219 suggests, however, that a large amount of Mn either (1) depresses the pigeonite to orthopyroxene inversion temperature so that the diffusion rate is lower and pigeonite is preserved by the sluggishness of the reaction or, (2) further increases the orthopyroxene nucleation energy

so that the manganiferous pigeonite has failed to invert because orthopyroxene was not nucleated.

Amphiboles

Cummingtonite. Cummingtonite is present throughout the iron formation and is an important constituent of most stratigraphic units. It occurs typically as prismatic grains which, in thin section, are colorless and have well-developed polysynthetic twinning. In some rocks it occurs as poikilitic grains enclosing quartz or magnetite. Orthopyroxene is present in most rocks which contain cummingtonite. Cummingtonites that have high Mg contents typically are poikilitic or prismatic and occur independently of orthopyroxene; in cummingtonites rich in Fe, however—especially those occurring with ferrohypersthene and fayalite—the cummingtonite grains generally are prismatic and directly replace associated fayalite or ferrohypersthene (Figs. 16 and 17). The replacement of ferrohypersthene by prismatic cummingtonite commonly appears to be volume-for-volume. Cummingtonites that have intermediate compositions commonly have an ambiguous textural relationship with associated orthopyroxenes; in a given rock some cummingtonites occur independently of the orthopyroxene grains whereas other cummingtonites clearly replace orthopyroxene.

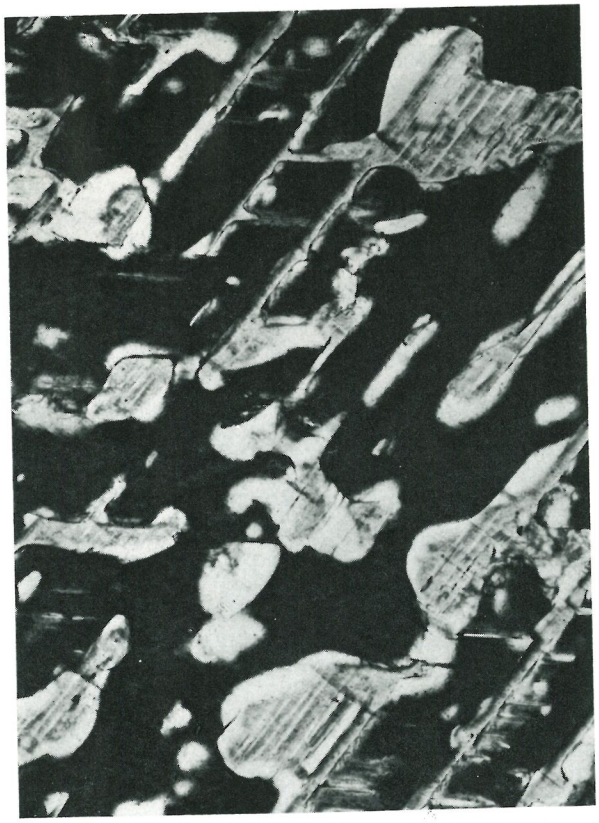

Fig. 15. A ferrohypersthene grain containing relict hedenbergite exsolution lamellae and blebs that had developed parallel to (001) in a former pigeonite grain. The hedenbergite blebs are believed to have formed during and immediately after the time of the pigeonite to ferrohypersthene inversion. Note that exsolution lamellae of Ca-poor pyroxene are present parallel to (001) within the hedenbergite blebs; it is not known if these lamellae are pigeonite or clinoferrohypersthene. (Crossed nicols, ×205)

Cummingtonites from a number of rocks were analyzed (Table 5). The compositions of early cummingtonites from rocks that lack orthopyroxene and cummingtonites that are believed to be in approximate equilibrium with orthopyroxene are included in Figure 4. In this figure it can be seen that all the early cummingtonites have Fe/(Mg+Fe) ratios of 60 percent or less. Cummingtonites which replace orthopyroxene or fayalite, however, have compositions that range from less than 30 percent to more than 70 percent Fe/(Mg+Fe). For all compositions, cummingtonites have lower Fe/(Mg+Fe) ratios than coexisting orthopyroxenes.

Cummingtonite occurs with quartz and magnetite throughout most of the iron formation. Only retrograde reactions involving small volumes of material among the three minerals have been observed; there is no indication of extensive prograde reactions having taken place. Late-stage, acicular cummingtonite replaces the margins of quartz grains that are in contact with orthopyroxene in some rocks (Figs. 17 and 18); also small cummingtonite grains have developed locally at the margins of a small proportion of the magnetite euhedra in quartz-rich layers. Secondary magnetite is present locally in areas which lack quartz, in association with cummingtonite that replaces orthopyroxene or fayalite (Fig. 16).

Many cummingtonite crystals are complex intergrowths of well-twinned colorless cummingtonite and untwinned cummingtonite that is pleochroic in various shades of green (Fig. 19). These complex grains are abundant in local coarse-grained areas such as at the boundary between a quartz-rich, and an orthopyroxene-rich magnetite layer or a magnetite-hedenbergite layer. Very fine, parallel hornblende exsolution lamellae are present in some untwinned green cummingtonites (Fig. 20). The untwinned green cummingtonites contain more Ca and Al than the colorless twinned grains. The grains containing very fine hornblende lamellae have the highest Al and Ca contents.

J. J. Papike (pers. commun.), U.S. Geological Survey, has determined the unit-cell dimensions of one of these untwinned green cummingtonites and of its enclosed hornblende exsolution lamellae (sample 026). These dimensions are:

	Cummingtonite	*Hornblende*
a	9.55±.03 Å	9.85±.03 Å
b	18.28±.05	18.14±.05
c	5.32±.02	5.32±.03
β	102°10′±10′	105°00′

Papike found that the optically visible hornblende lamellae are located along the $(10\bar{1})$ plane of the host cummingtonite and that, in addition, the cummingtonite contains hornblende lamellae which can not be resolved optically along the (100) plane.

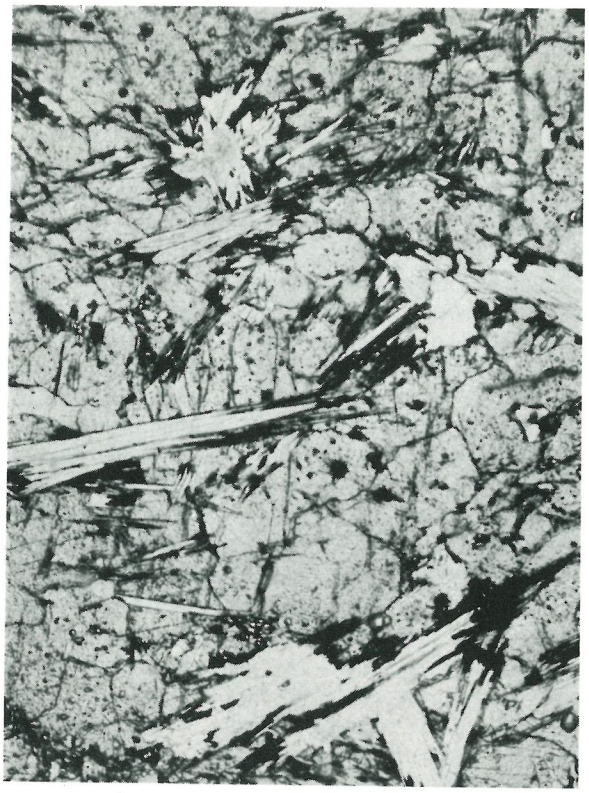

FIG. 16. Nearly monomineralic fayalite being replaced by prismatic cummingtonite. Secondary magnetite (black) is developed at the margins of some of the cummingtonite grains. (Plane light, ×31)

The cummingtonites whose weight percent of Al_2O_3 was measured are included in Figure 22, together with hornblendes. In this figure it can be seen that cummingtonites in two rocks (026 and 088) have relatively high Al_2O_3 contents. Cummingtonite 026a contains hornblende exsolution lamellae. In sample 088, cummingtonite (a) consists of subhedral grains that are untwinned and brown in thin section. They are approximately contemporaneous with the almandine garnet, fayalite and ferrohypersthene in the rock but evidently were not stable during cooling. These cummingtonite grains, especially their outer portions, are partially to completely replaced by the more magnesian type (b) of cummingtonite. Type (b) cummingtonite is colorless and twinned and the grains are surrounded by heavy rims of secondary magnetite.

More than one generation of cummingtonite is present in many rocks, the later stages generally have higher Fe/(Mg+Fe) ratios and are finer-grained. If poikilitic grains are present, they generally are earlier than prismatic grains; these, in turn, are earlier than any fibrous and acicular cummingtonite that may be present.

Hornblende. Hornblende is widely distributed in the iron formation but is not as abundant as pyroxenes, fayalite, or cummingtonite. The hornblende in some rocks is contemporaneous with coexisting pyroxenes and fayalite but, most commonly, it replaces Ca pyroxene.

Early hornblendes commonly are subhedral or euhedral and occur mainly in quartz-rich layers and in layers rich in hornblende; rarely they are poikilitic. Early hornblendes in an individual rock generally are uniform in color and composition.

Hornblende which replaces Ca pyroxene has developed mainly at the margins of grains, generally adjacent to quartz. Where this replacement is strongly developed, small patches of hornblende can be identified throughout the Ca pyroxene grains. In some of the rocks which lack orthopyroxene and cummingtonite, the replacement of Ca pyroxene by hornblende was accompanied by the development of abundant calcite. Hornblende commonly is present adjacent to magnetite euhedra in quartz-rich layers and commonly replaces Ca pyroxene adjacent to magnetite grains and laminae. In a few rocks poikilitic and interstitial hornblende grains have developed along grain boundaries of other minerals such as orthopyroxene or plagioclase. Coarse-grained replacement patches and incipient pegmatites of hornblende are present in local stratigraphic zones; these texturally are similar to cross-cutting pegmatite veins that contain iron-rich hornblende.

In some quartz-magnetite rocks both early and late hornblende grains are present. In such rocks, the hornblende consists of an assortment of independent prismatic grains, interstitial grains, and grains at the margins of Ca pyroxene and magnetite grains. These hornblendes gener-

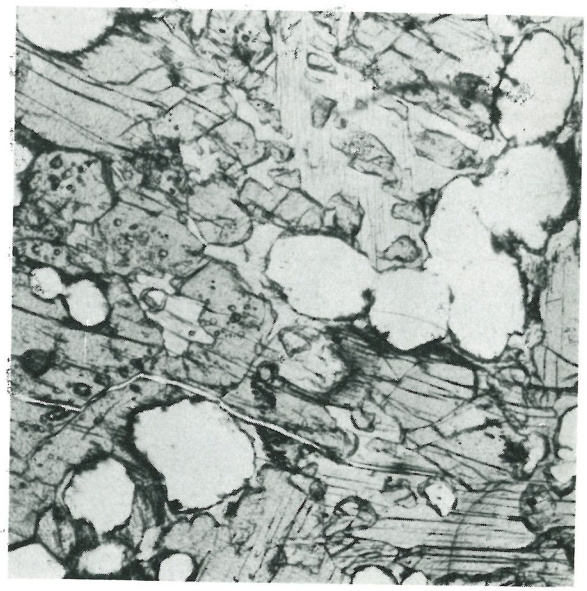

FIG. 17. Poikilitic orthopyroxene enclosing rounded quartz grains. Note the volume-for-volume replacement of orthopyroxene by prismatic cummingtonite (grey, lower relief than orthopyroxene). The dark areas at the edges of some of the quartz grains are very fine late-stage cummingtonite fibers. (Plane light, ×37)

TABLE 5. COMPOSITIONS OF CUMMINGTONITES

Sample Number	Wt %							Atomic proportions		Comments
	MgO	FeO	CaO	MnO	Al_2O_3	SiO_2	Total	Mg / Mg+Fe+Ca	Fe / Mg+Fe+Ca	
017	14.0	28.0	1.7	—	—	—	43.7	0.453	0.508	Prismatic grains marginal to coarse hornblende
026 (a)	9.5	33.7	1.5	0.4	2.3	50.3	97.7	.322	.641	Untwinned with hornblende lamellae, replaces ferrohypersthene
(b)	9.3	35.7	0.8	0.5	0.7	51.5	98.5	.311	.670	Volume-for-volume replacement of ferrohypersthene
(c)	5.7	39.7	0.5	0.6	0.4	51.6	98.5	.201	.786	Late fibrous grains with secondary magnetite
073	12.5	30.0	1.3	—	—	—	43.8	.413	.556	Mainly independent poikilitic grains
082	8.0	37.0	0.5	0.4	—	52.0	97.9	.275	.713	Minor replacement of ferrohypersthene
087	7.5	36.5	0.4	1.3	—	52.0	97.7	.265	.725	Mainly replaces ferrohypersthene
088 (a)	11.0	30.5	1.0	0.8	4.8	—	48.1	.381	.594	Early grains
(b)	13.0	31.0	0.3	0.8	1.9	—	47.0	.425	.568	Replaces (a) and late grains with secondary magnetite rims
122 (a)	7.4	38.9	1.1	0.3	0.8	52.7	101.2	.247	.727	Volume-for-volume replacement of ferrohypersthene
(b)	8.9	34.3	0.9	0.3	b.v.	53.3	97.7	.309	.669	Replaces fayalite with secondary magnetite
(c)	4.7	41.6	0.8	0.3	0.7	52.1	100.2	.164	.816	Late fibrous grains
131 (a)	24.5	16.5	0.6	0.2	0.8	58.0	100.6	.716	.271	Early poikilitic grains
(b)	24.0	17.0	1.3	0.2	1.2	58.0	101.7	.696	.277	Late prismatic grains, some replace hypersthene
145 (a)	12.8	28.0	1.4	—	—	—	42.2	.434	.532	Average composition
(b)	14.2	26.3	1.9	—	—	—	42.4	.468	.487	Green untwinned grains with hornblende lamellae
(c)	11.4	29.3	1.1	—	—	—	41.8	.398	.574	Colorless well-twinned grains
175	9.0	33.5	0.8	—	—	—	43.3	.317	.663	Mainly replaces fayalite with secondary magnetite
208	9.2	31.9	1.0	—	—	—	42.1	.331	.643	Replaces ferrohypersthene
219	4.0	35.0	1.2	7.5	b.v.	51.0	98.7	.163	.802	Replaces Mn pigeonite
234	6.9	35.6	—	1.5	0.8	51.2	96.0	.257	.743	Replaces fayalite
241	9.0	31.0	1.1	2.5	0.7	52.0	96.3	.331	.640	Replaces ferrohypersthene and intergrown with hornblende
266	11.5	30.0	1.2	2.8	0.6	52.0	98.1	.394	.577	Independent grains and replaces ferrohypersthene
304	21.0	20.5	1.0	—	—	—	42.5	.632	.346	Replaces hypersthene
343	12.0	30.5	1.5	1.7	0.3	54.0	100.0	.397	.567	Independent grains

ally have relatively low Al_2O_3 contents and show more compositional variation than in rocks where all the hornblende definitely is early; but not as much variation as in rocks where all the hornblende definitely is late. Cummingtonite commonly is present as a similar mixture of early and late grains in the same rocks.

The latest Ca amphiboles are fine-grained, brown, and acicular; they have grown into quartz from the edges of earlier hornblende grains or rarely from cummingtonite. These are present in some samples of quartz-hedenbergite-magnetite taconite that contains abundant late hornblende replacing Ca pyroxene. The composition of the acicular Ca amphibole was measured in samples 145 and 149; iron is substantially more abundant than in the associated hornblende grains in both, and the compositions are quite variable from one point to another.

In sample 149 the acicular Ca amphibole averages 92 percent Fe/(Mg+Fe); this is much richer in Fe than any other Ca amphibole whose composition was measured. In addition, the Al_2O_3 content is much lower than that of the other Ca amphiboles. This mineral's composition is close to ferrotremolite, the theoretical iron end member of the tremolite-actinolite series, and it can be called ferroactinolite.

Hornblendes from several rocks were analyzed (Table 6); their atomic proportions of Mg, Fe, and Ca are plotted in Figure 21, together with coexisting Ca pyroxene compositions. Nearly all the hornblendes contain less Ca than the 28.6 atom percent of Ca/(Mg+Fe+Ca) in the ideal $Ca_2(Fe,Mg)_5Si_8O_{22}(OH)_2$ formula of actinolite. In general, hornblendes from rocks with neither orthopyroxene nor cummingtonite have higher (closer to ideal) Ca contents.

Two compositional stages of Ca amphibole were mea-

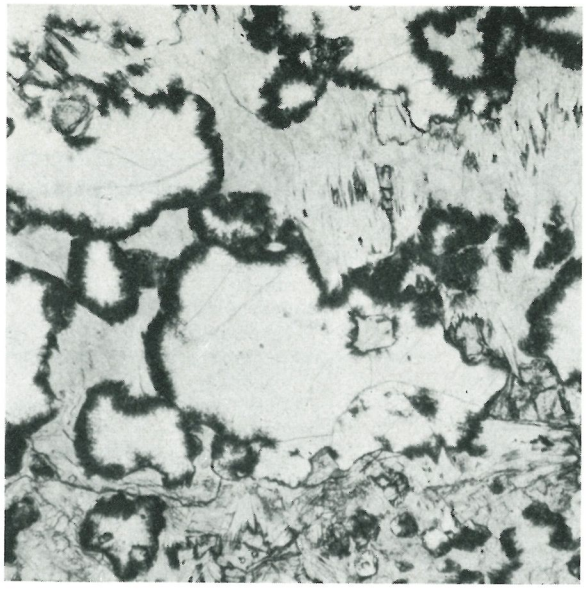

FIG. 18. Masses of fine-grained prismatic and fibrous cummingtonite (grey, moderate relief) and surrounding rims of acicular cummingtonite (dark-colored) developed in a quartz-rich layer at its boundary with a layer of ferrohypersthene-fayalite taconite. (Plane light, ×32)

sured in samples 134, 140, 145, and 149; in all four rocks the later grains contain a higher proportion of Fe (the ferroactinolite of sample 149 is too rich in Fe to be shown on Figure 21).

In Figure 22 the weight percent of Al_2O_3 is plotted against the atom percent of Fe/(Mg+Fe) for all hornblendes and cummingtonites whose Al_2O_3 content was measured. The wide variations in the Al_2O_3 content of many of the late hornblendes are shown in this figure. These variations, along with the grain to grain variations in a given rock and variations within individual grains indicate that, in general, late hornblendes have lower amounts of Al_2O_3 than early hornblendes for a specific Fe/(Mg+Fe) ratio. For early hornblendes, the Al_2O_3 content, increases as the Fe/(Mg+Fe) ratio increases. Evidently, as the temperature decreased, hornblendes containing lower and lower amounts of Al were able to form for a specific Fe/(Mg+Fe) ratio.

Equilibrium relationships. Cummingtonites that are contemporaneous with pyroxenes contain 60 percent or less Fe/(Mg+Fe); cummingtonites with higher Fe/(Mg+Fe) ratios formed only as the temperature was lowered. This composition, the compositions of coexisting orthopyroxenes (Fig. 4), and the relationships among pyroxenes and fayalite plus quartz proposed in Figure 7 are the basis for Figure 23 which shows the equilibrium relationships proposed between cummingtonite and coexisting pyroxenes at the maximum temperature and other conditions attained during metamorphism.

Because much of the cummingtonite has more than 60 percent Fe/(Mg+Fe) and is later than associated pyroxenes, it is suggested that at lower temperatures the cummingtonite field extends farther toward the Fe-rich side of Figure 23. This interpretation is in agreement with relationships between orthopyroxene and cummingtonite shown on temperature-composition diagrams for the join $Mg_3Si_4O_{10}(OH)_2$—$Fe_3Si_4O_{10}(OH)_2$ by Boyd (1959) and Kranck (1961). An increase in the activity of H_2O would have the same result on the maximum Fe/(Mg+Fe) ratio of cummingtonite that could form contemporaneously with orthopyroxene as would decreasing the temperature.

At some lower temperature, cummingtonite would be in equilibrium with both ferrohypersthene and fayalite plus quartz (a thermodynamic invarient point, if total pressure and activity of H_2O are specified). At still lower temperatures, ferrohypersthene and fayalite plus quartz would combine with any H_2O remaining in the rock to form late cummingtonite. Cummingtonite formed from ferrohypersthene that coexists with fayalite plus quartz normally contains 70–75 percent Fe/(Mg+Fe). Cummingtonite formed at lower temperatures may be even richer in Fe; compositions close to 85 percent Fe/(Mg+Fe) were measured with some of the very late fibrous cummingtonites.

The compositions of both early and late hornblendes span the range of Fe/(Mg+Fe) ratios that is available in the iron formation. The hornblendes contain several per-

FIG. 19. A portion of a cummingtonite grain that varies from colorless and well-twinned (light grey) to untwinned and pleochroic in various shades of green (medium grey). Small remnants of altered Ca pyroxene (high relief) are present within the cummingtonite and acicular cummingtonite fibers have grown at the edges of the quartz. (Plane light, ×64)

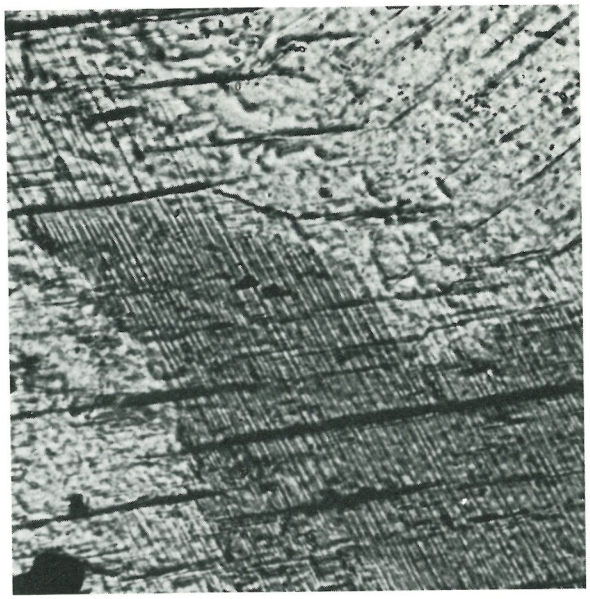

FIG. 20. Very thin hornblende exsolution lamellae (thin striations) in the cummingtonite grain of Figure 19. The hornblende exsolution lamellae occur principally in the untwinned green areas (dark) of the cummingtonite. (Plane light, ×306)

cent of Al_2O_3. As indicated previously, in a particular rock or for a specific Fe/(Mg+Fe) ratio, late hornblendes generally contain less Al_2O_3 than early ones. For hornblendes that are approximately contemporaneous with coexisting pyroxenes, there is a general increase in the weight percent of Al_2O_3 that coincides with an increase in the Fe/(Mg+Fe) ratio (Fig. 22).

The above observations and the relationships proposed in Figure 7 for coexisting pyroxenes and fayalite plus quartz, suggest the relationships proposed in Figure 24 for hornblende coexisting with pyroxenes and fayalite plus quartz at the maximum temperature and other conditions

TABLE 6. COMPOSITIONS OF HORNBLENDES

Sample Number	Wt %							Atomic Proportions		Comments
	MgO	FeO	CaO	MnO	Al_2O_3	SiO_2	Total	Mg/(Mg+Fe+Ca)	Fe/(Mg+Fe+Ca)	
017	11.5	20.0	10.5	—	—	—	42.0	0.380	0.371	Early poikilitic grains
122	6.2	27.6	9.9	0.2	5.8	49.2	98.9	.215	.538	Replaces hedenbergite and plagioclase
131	17.5	11.5	10.0	0.1	7.0	52.0	98.1	.562	.207	Early grains
134 (a)	10.3	20.2	12.4	1.2	6.6	—	50.7	.337	.371	Early, enclosed in garnet
(b)	6.7	24.4	11.8	1.1	9.1	—	53.1	.232	.474	Late, replaces Ca pyroxene
140 (a)	12.0	18.0	10.0	1.3	7.5	48.0	96.8	.410	.345	Early, separate lamina
(b)	11.5	19.5	10.0	1.1	7.0	48.0	97.1	.388	.369	Late, interstitial to ferrohypersthene
142	7.5	22.5	9.0	0.8	9.3	—	49.1	.282	.475	Late, replaces hedenbergite next to magnetite
145 (a)	11.3	19.6	9.4	—	—	—	40.3	.389	.378	Early grains, late grains replacing Ca pyroxene next to magnetite
(b)	6.2	24.8	9.6	—	—	—	40.6	.230	.515	Late fibers at edges of (a)
149 (a)	6.0	24.5	11.0	1.3	6.5	—	49.3	.217	.497	Replaces hedenbergite and developed in quartz lamina
(b)	1.5	31.0	11.5	1.5	0.5	—	46.0	.055	.641	Ferroactinolite, late fibers at edges of (a)
173	5.5	25.5	10.5	0.7	6.0	—	48.2	.201	.523	Replaces hedenbergite
210	6.1	24.8	10.3	—	—	—	41.2	.222	.508	Replaces hedenbergite
234	5.2	26.3	10.2	0.7	10.2	38.5	91.1	.190	.541	Early grains
241	6.5	25.0	10.0	1.1	9.0	42.0	93.6	.235	.506	Late pegmatitic area
262[a]	5.14	27.28	11.12	1.98	4.91	46.40	100.11	.181	.538	Pegmatitic vein, wet chemical analysis
266	10.5	21.5	9.5	1.1	2.4	52.0	97.0	.357	.411	Independent grains and replaces Ca pyroxene
304	15.5	12.0	11.5	0.2	3.6	56.8	99.6	.508	.221	Mainly early grains
343	10.5	21.5	9.5	0.8	2.5	50.5	95.3	.357	.411	Independent grains and replaces Ca pyroxene

[a] FeO consists of 24.44 percent FeO and 3.16 percent Fe_2O_3 reported as FeO; the total includes 0.49 percent Na_2O, 0.47 K_2O, 1.80 H_2O+, 0.01 P_2O_5, 0.08 F and 0.19 Cl less O=F, Cl of 0.08. The analysis indicates 0.00 H_2O-, 0.00 TiO_2 and 0.00 CO_2 are present. (L. E. Reichen, analyst).

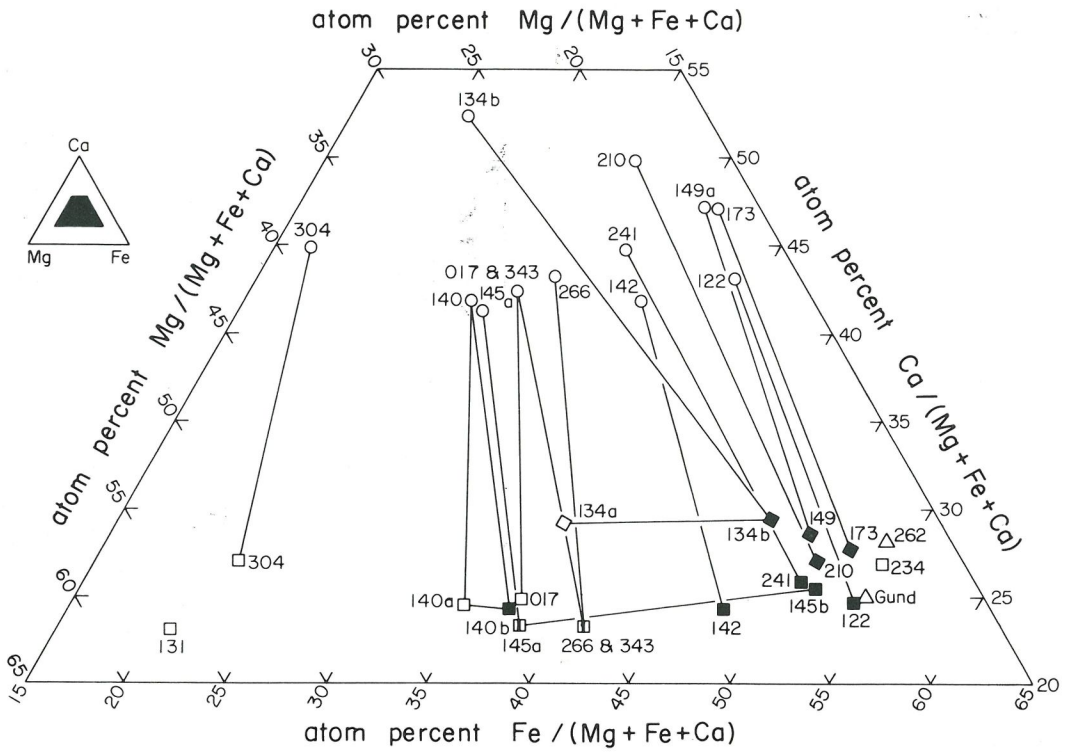

□ ◫ ■ hornblendes from rocks that contain Ca-poor pyroxene or cummingtonite (Only cummingtonite is present in samples 017, 145, and 343; sample 234 coexists with fayalite and ferrohypersthene.)

◇ ◆ hornblendes from rocks which lack orthopyroxene and cummingtonite

△ hornblendes from pegmatitic veins; the one labeled (Gund) was reported by Gundersen and Schwartz (1962)

○ Ca pyroxenes that coexist with these hornblendes

Open symbols: hornblendes that are approximately contemporaneous with the coexisting silicate minerals

Filled symbols: hornblendes that are later than the coexisting Ca pyroxene

Vertical bar: ambiguous time relationship between coexisting hornblende and Ca pyroxene

FIG. 21. Compositions of hornblendes and associated Ca pyroxenes from the Eastern Mesabi district.

attained during metamorphism. The heavy line labeled hornblende and T_E-T_E' represents the minimum permissible amount of Al_2O_3 for the compositions of early hornblendes. The end point, T_E, of this line corresponds approximately to the composition of the hornblende that coexists with ferrohypersthene and fayalite plus quartz in sample 234; it contains 10.2 weight percent of Al_2O_3. The manner in which this minimum Al_2O_3 line and the tie lines are drawn

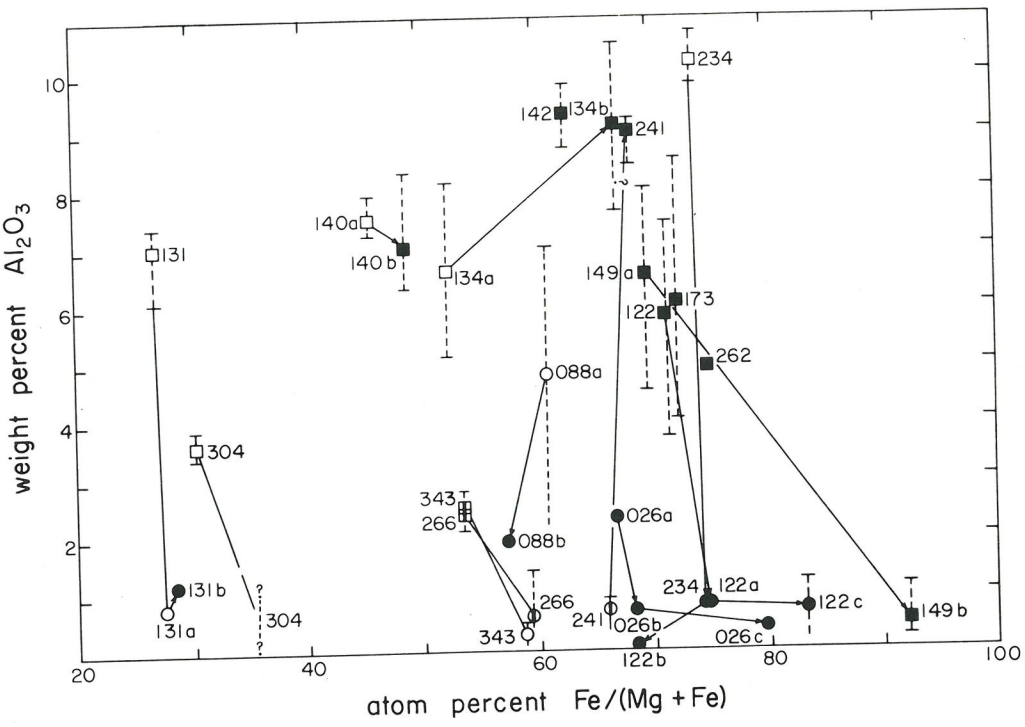

FIG. 22. Plot of weight % Al_2O_3 versus atom % Fe/(Mg + Fe) for cummingtonites and hornblendes from the Dunka River area. Arrowheads on the ends of some tie lines indicate the sequence of formation. The range of Al_2O_3 % in hornblendes from an individual rock is indicated by the vertical dashed line. Cummingtonite is present in sample 304, however its Al_2O_3 content was not measured. Sample 149(b) is a late acicular ferroactinolite overgrowth on hornblende grains.

in relation to the pyroxene quadrilateral is consistent with the mineral compositions obtained in this study; however, these relationships are proposed as only a tentative suggestion. Additional analyses of coexisting minerals are necessary for either confirmation or modification.

The apparent decrease in the amount of Al_2O_3 necessary to stabilize hornblende as the temperature decreases, suggests that at some lower temperature the minimum amount of Al_2O_3 necessary would be approximately that given by the heavy dashed line, T_L-T_L'. The position of line T_L-T_L' is lowered with decreasing temperature. At temperatures of crystallization below those attained in the Dunka River area, actinolite containing virtually no Al could form in the same range of Fe/(Mg+Fe) ratios. Such temperatures were probably attained at Mt. Wright, Quebec, where Ca amphiboles are abundant in a metamorphosed iron formation, but the highest Al content reported is 1.2 weight percent Al_2O_3 (Mueller, 1960).

Although the relationships proposed between temperature, Fe/(Mg+Fe) ratios, and minimum permissible content of Al_2O_3 in hornblende are tentative, little doubt exists that hornblende has formed contemporaneously with pyroxenes through the complete range of Fe/(Mg+Fe) ratios found in the Dunka River rocks, and with fayalite plus quartz at the iron-rich end of this range.

The compositional relationships suggested in Figures 23 and 24 for cummingtonite and hornblende coexisting with pyroxenes and fayalite plus quartz are combined to form Figure 25, which shows equilibrium relationships proposed among these minerals at the maximum temperature and other conditions attained during metamorphism. In rocks that have sufficient Mg the four solid solution minerals—Ca pyroxene, orthopyroxene, hornblende, and cummingtonite—were able to crystallize contemporaneously; however, in rocks richer in Fe, cummingtonite was able to form only during retrograde metamorphism.

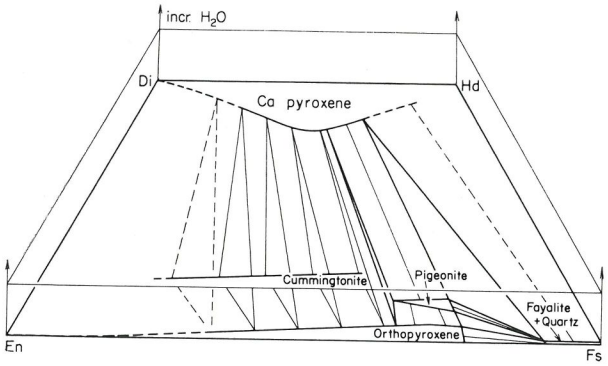

FIG. 23. Equilibrium phase relationships proposed to hold for cummingtonite coexisting with pyroxenes at the maximum temperature (700°–750°C.) and other conditions attained during metamorphism of the Biwabik Iron Formation in the Dunka River area.

Replacement of orthopyroxene and fayalite by cummingtonite. For rocks in which the composition of the replaced ferrohypersthene or fayalite and the replacing cummingtonite are known, balanced equations can be written which approximate the reactions that occurred. For example, in sample 122 cummingtonite (b) that has 68.4 percent Fe/(Mg+Fe) replaces fayalite that has 91.2 percent Fe/(Mg+Fe) and is accompanied by abundant secondary magnetite. A balanced equation for this reation is:

$$12.58(Fe_{0.912}Mg_{0.088})_2SiO_4 + H_2O + 3O_2 \rightarrow$$
$$(Fe_{0.684}Mg_{0.316})_7Si_8O_{22}(OH)_2 + 4.58SiO_2 + 6.04Fe_3O_4$$

To balance this equation it was assumed that the amount of Mg remained constant and that it is entirely confined to the silicate minerals. It is also assumed that the affect of any Al, Ca, Mn, and other elements which may be present is negligible, that all the Fe in fayalite and cummingtonite is in the ferrous state, that the minerals have stochiometric ratios of FeO plus MgO to SiO_2, and that the reaction as written with the consumption of H_2O and O_2 and the liberation of SiO_2 and Fe_3O_4 is correct.

For similar reactions, an excess of Fe beyond that in the silicates usually is present on either the reactants or products side. If expressed as Fe_3O_4, as in the example, the addition of O_2 is required on the other side of the reaction for balancing. Generally, however, magnetite is not observed to be present and evidently was not involved except in a few cases such as the example. Consequently, it is more convenient to express the excess iron as FeO rather than Fe_3O_4 so that free oxygen is not required.

By varying the Fe/(Mg+Fe) ratios of the cummingtonite and fayalite independently, a number of ways are seen by which a balanced reaction between the two silicates can be written; SiO_2 and FeO may appear together or on opposite sides of the reaction, or one may not be involved in the reaction. These various modifications of the fayalite to cummingtonite reaction are illustrated on the FeO-MgO-SiO_2 plane in Figure 26. The five equations that apply to the five regions labeled A, B, C, D, and E, in this figure are:

A. fayalite + H_2O → cummingtonite + SiO_2 + FeO
B. fayalite + H_2O → cummingtonite + FeO
C. fayalite + SiO_2 + H_2O → cummingtonite + FeO
D. fayalite + SiO_2 + H_2O → cummingtonite
E. fayalite + SiO_2 + FeO + H_2O → cummingtonite

The following, similar set of reactions for the replacement of orthopyroxene by cummingtonite, could be illustrated in the same manner.

A. orthopyroxene + H_2O → cummingtonite + SiO_2 + FeO

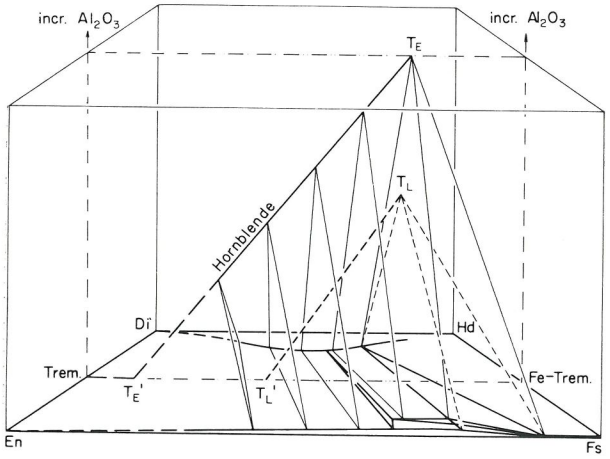

FIG. 24. Equilibrium phase relationships tentatively proposed to hold for hornblende coexisting with pyroxenes and fayalite plus quartz during the metamorphism of the Biwabik Iron Formation in the Dunka River area. See text for explanation.

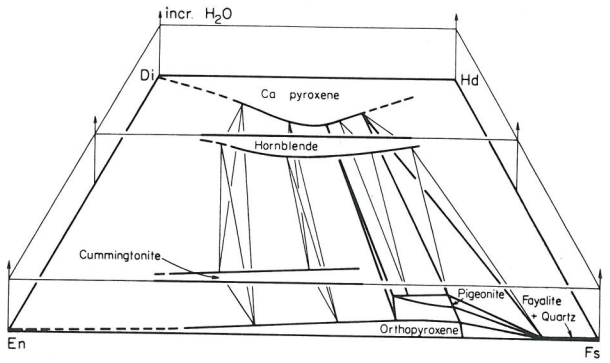

FIG. 25. Equilibrium phase relationships tentatively proposed to hold among amphiboles, pyroxenes, and fayalite plus quartz at the maximum temperature (700°–750°C.) and other conditions prevailing during the metamorphism of the Biwabik Iron Formation in the Dunka River area.

B. orthopyroxene + H_2O → cummingtonite + FeO

C. orthopyroxene + SiO_2 + H_2O → cummingtonite + FeO

D. orthopyroxene + SiO_2 + H_2O → cummingtonite

E. orthopyroxene + SiO_2 + FeO + H_2O → cummingtonite

The compositions of fayalite, ferrohypersthene, and cummingtonite that were measured in sample 122 are plotted in Figure 27. This sample consists of several quartz-rich layers that are interbedded with laminated silicate-rich beds. The ferrohypersthene is coarse-grained and has inverted from pigeonite; the fayalite grains are concentrated mainly in laminae with hedenbergite. Three types of cummingtonite are present:

1. Type (a), prismatic grains replacing ferrohypersthene on what appears to be a volume-for-volume basis, and locally replacing fayalite. These grains generally are isolated from one another and are not accompanied by secondary magnetite.

2. Type (b), prismatic grains similar to those of type (a), but accompanied by abundant secondary magnetite, replace some fayalite grains. These grains are adjacent to a serpentine vein in an area lacking visible quartz.

3. Type (c), very fine-grained prismatic to acicular cummingtonite is strongly developed at the edges of the quartz-rich layers, adjacent to ferrohypersthene laminae (Fig. 18). Patches and veinlets of this type of cummingtonite also are developed throughout the ferrohypersthene grains. The Fe/(Mg+Fe) ratio of this type is quite variable but does not overlap that of type (a).

From Figure 27 it can be seen that the replacement of ferrohypersthene by type (a) cummingtonite is reasonably approximated by reaction B (ferrohypersthene + H_2O → cummingtonite + FeO), in which SiO_2 is neither liberated nor consumed. FeO, however, has been liberated and, as it is not precipitated as magnetite, evidently was removed from the reaction site.

Fayalite is replaced by prismatic cummingtonite that has the type (a) composition where quartz is present, and ranges to the type (b) composition in areas containing abundant secondary magnetite but no quartz. The replacement of fayalite by cummingtonite does not appear to be volume-for-volume.

In Figure 27, the replacement of fayalite by cummingtonite (a) is seen to be approximated best by reaction A (fayalite + H_2O → cummingtonite + SiO_2 + FeO) and for type (b) cummingtonite, by (fayalite + H_2O + O_2 → cummingtonite + SiO_2 + magnetite), as indicated previously.

The replacement of ferrohypersthene by type (c) cummingtonite has the form of reaction E (ferrohypersthene + SiO_2 + FeO + H_2O → cummingtonite); or locally, where sufficient Mg is present, the reaction is D which involves no gain or loss of Fe.

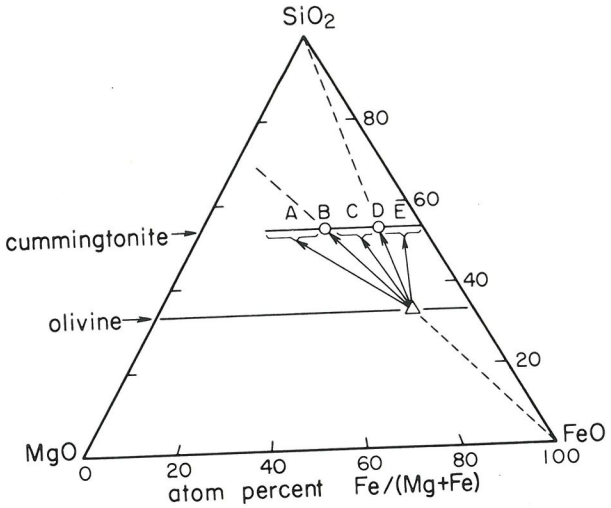

FIG. 26. Graphical representation of some possible reactions for fayalite that has a specific composition being replaced by cummingtonites of various compositions. See text for reactions and explanation.

From the above discussion, it is evident that cummingtonite has replaced ferrohypersthene by two distinct reactions in the same rock. During the volume-for-volume replacement by type (a), iron was liberated but the SiO_2 content evidently was not changed significantly; however, during the later formation of fibrous and acicular type (c) cummingtonite both iron and SiO_2 were consumed. As both types of cummingtonite are developed in close proximity to one another, it seems probable that the iron liberated during the growth of type (a) was consumed by the growth of type (c). The need for SiO_2 most likely has caused the localization of type (c) at the junction of ferrohypersthene-rich and quartz-rich laminae and at the edges of quartz inclusions in ferrohypersthene. Locally, type (c) replaces type (a) and has grown into quartz grains adjacent to type (a).

Ferrohypersthene evidently was replaced on a volume-for-volume basis by prismatic cummingtonite in many rocks; the reaction is closely approximated by reaction B (ferrohypersthene + H_2O → cummingtonite + FeO), as in sample 122. Such cummingtonite has preserved the Mg/Si ratio of the parent orthopyroxene. This type of replacement may have resulted from an ionic exchange between ferrohypersthene and the residual intergranular fluid which remained in the rock after prograde metamorphism; the exchange actually may be as simple as:

$$\text{orthopyroxene} + 2H^+ \rightarrow \text{cummingtonite} + Fe^{2+}$$

Fibrous and acicular cummingtonite is common in some rocks between ferrohypersthene and quartz grains (Fig. 17), along veinlets, and between quartz-rich and ferrohy-

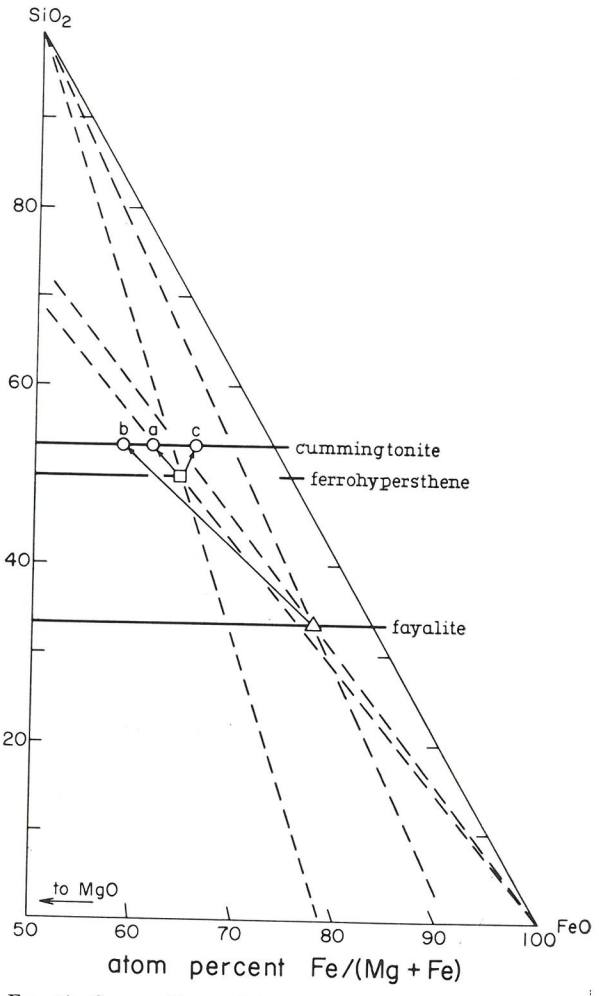

FIG. 27. Compositions of fayalite, ferrohypersthene, and three generations of cummingtonite from sample 122. See text for explanation.

persthene- or fayalite-rich laminae, as in sample 122 (Fig. 18). It most likely was formed from the ferromagnesian minerals with the addition of SiO_2 supplied by local quartz and H_2O and minor quantities of Fe from the residual intergranular fluid. Such cummingtonite could form in local areas of a rock until the residual H_2O was exhausted along nearby grain boundaries.

The replacement of fayalite by prismatic cummingtonite does not appear to be volume-for-volume; this probably reflects the great difference between cummingtonite and fayalite in crystalline structure, whereas there is a similarity in the structures of orthopyroxene and cummingtonite. Evidently both iron and SiO_2 are liberated during this reaction. Secondary magnetite (Fig. 16) locally is present; it occurs most commonly as described in sample 122, accompanying prismatic cummingtonite which replaces fayalite in areas where quartz is absent and evidently has formed by a reaction similar to: (fayalite + H_2O + O_2 → cummingtonite + SiO_2 + magnetite). Secondary magnetite also has developed approximately contemporaneously with very late-stage Fe-rich fibrous and acicular cummingtonite that occurs mainly in patches and veins. On the basis of compositions, this type of late cummingtonite evidently has formed by a reaction of type E (ferrohypersthene + SiO_2 + FeO + H_2O → cummingtonite). Oxygen evidently was available so that some of the Fe associated with the residual intergranular H_2O was precipitated as magnetite.

ACKNOWLEDGEMENTS

The writer gratefully acknowledges Paul Sims, Director of the Minnesota Geological Survey, for suggesting the problem and for making the initial arrangements for its pursuance. Paul Weiblen was kind enough to instruct the writer on the operation of the electron microprobe. The wet chemical analyses of samples 262 and 330 were provided by the U.S. Geological Survey; the analyses were arranged for, and the mineral separations carried out under the direction of Rolland L. Blake of the U.S. Bureau of Mines. The unit cell dimensions for the amphiboles in sample 026 were determined by J. J. Papike of the U.S. Geological Survey.

Financial support during part of this study was provided by a Reserve Mining Company Fellowship and by the Minnesota Geological Survey. This study would not have been possible without the full cooperation of Erie Mining Co.

REFERENCES

BINNS, R. A., J. V. P. LONG, AND S. J. B. REED (1963) Some naturally occurring members of the clinoenstatite-clinoferrosilite mineral series. *Nature* **198,** 777–778.

BONNICHSEN, B. (1968) *General geology and petrology of the metamorphosed Biwabik Iron Formation, Dunka River area, Minnesota.* Ph.D. thesis, Univ. of Minn., 240 pp.

BOWN, M. G., AND P. GAY (1960) An X-ray study of exsolution phenomena in the Skaergaard pyroxenes. *Mineral Mag.* **32,** 379–388.

BOYD, F. R. (1959) Hydrothermal investigations of amphiboles. In P. H. Abelson (Ed.), *Researches in Geochemistry,* John Wiley and Sons, New York, p. 377–396.

———, AND J. F. SCHAIRER (1964) The system $MgSiO_3$-$CaMgSi_2O_6$. *J. Petrology* **5,** 275–309.

BROWN, G. M. (1957) Pyroxenes from the early and middle stages of fractionation of the Skaergaard intrusion, East Greenland. *Mineral. Mag.* **31,** 511–543.

DALLWITZ, W. B., D. H. GREEN, AND J. E. THOMPSON (1966) Clinoenstatite in a volcanic rock from the Cape Vogel area, Papua. *J. Petrology* **7,** 375–403.

GUNDERSEN, J. N., AND G. M. SCHWARTZ (1962) The geology of the metamorphosed Biwabik Iron Formation, Eastern Mesabi district, Minnesota. *Minn. Geol. Surv. Bull.* **43,** 139 pp.

KRANCK, S. H. (1961) A study of phase equilibria in a metamorphic iron formation. *J. Petrology* **2,** 137–184.

KUNO, H. (1966) Review of pyroxene relations in terrestrial rocks in the light of recent experimental works. *Mineral. J. (Jap.)* **5,** 21–43.

MUELLER, R. F. (1960) Compositional characteristics and

equilibrium relations in mineral assemblages of a metamorphosed iron formation. *Amer. J. Sci.* **258,** 449–497.

MUIR, I. D. (1954) Crystallization of pyroxenes in an iron-rich diabase from Minnesota. *Mineral. Mag.* **30,** 376–388.

O'NEIL, J. R., AND R. N. CLAYTON (1964) Oxygen isotope geothermometry. In *Isotopic and Cosmic Chemistry, Urey Volume,* North Holland, p. 157–168.

PERRY, E. C., JR., AND B. BONNICHSEN (1966) Quartz and magnetite: oxygen-18-oxygen-16 fractionation in metamorphosed Biwabik Iron Formation. *Science* **153,** 528–529.

———, AND J. W. MORSE (1967) Oxygen isotopic evidence of metamorphism in the Biwabik Iron Formation, Minnesota (abstr.). *13th Ann. Inst. L. Superior Geol.*

POLDERVAART, A., AND H. H. HESS (1951) Pyroxenes in the crystallization of basaltic magma. *J. Geol.* **59,** 472–489.

WHITE, D. A. (1954) The stratigraphy and structure of the Mesabi range, Minnesota. *Minn. Geol. Surv. Bull.* **38,** 92 pp.